Quantitative Determination of Surface Markers on B-cell Chronic Lymphocytic Leukemia (CLL) Cells

Suli Niu

Thesis submitted to the

Faculty of Graduate and Postdoctoral Studies

in partial fulfillment of the requirements

for the M.A.Sc. degree in Chemical Engineering

Department of Chemical and Biological Engineering

Faculty of Engineering

University of Ottawa

ABSTRACT

To supplement and modify the diagnosis and clinical research of B-cell Chronic Lymphocytic Leukemia (B-CLL), a new method based on cell imaging and image processing was developed and applied to the B-CLL patient samples. The fluorophore-labelled leukemia cells were clearly visualized, reflecting the positive/negative expression of the corresponding surface markers and their distribution. Computer algorithms were devised and used to analyze a large number of images. The fluorescence intensity of the labelled antibodies on a given cell directly reflects the expression of the corresponding surface markers. The morphology and size of leukemia cells were not identical even in the same patient's sample and the size variation does not correlate with the number of surface markers. The amount of each surface marker was approximately fixed for each patient, but there were some relationships, for instance, the number of CD19 and CD38 markers were correlated to each other. The heterogeneous expression of surface markers confirmed an assumption that surface markers have their preferred membrane positions. One of the most important results is that the cell imaging and our image processing method has provided an alternative and reliable way to diagnose B-CLL and new insights in the prognosis of subtype of B-CLL.

ACKNOWLEDGEMENTS

All research described in this thesis could not be possible without the help of many people. First of all, I sincerely thank Dr. Shan Zou and Dr. Pierre Berini, my supervisors, to give me the opportunity to get involved in this great project. Also please allow me to thank you for your patience and understanding when I was confused, and thanks for your professional and knowledgeable help to show me the direction.

Many thanks also to Dr. Maohui Chen and Dr. Zhengfang Lu, for their professional guidance. Without their help, the project results would not be as successful as they are. I would also want to thank everyone in Dr. Linda Johnston's group. They provided such a friendly and helpful research environment. I enjoyed my stay at the NRC and missed those days very much.

Please let me show my special thanks to Dr. Chen Wang. Thanks for your samples and advice. They were the key of this project. Also, thanks to the BiopSys NSERC Strategic Network for Bioplasmonic Systems, for the funding support.

TABLE OF CONTENTS

LIST OF TABLE

LIST OF FIGURES

LIST OF ABBREVIATIONS

B-CLL: B-cell Chronic Lymphocytic Leukemia

CD: Cluster of Differentiation

FITC: Fluorescein Isothiocyanate

PE: R-phycoerythrin

PC7: R-phycoerythrin-Cyanine 7

Cy5: Cyanine 5

FCS: Fetal Calf Serum

PBS: Phosphate Buffered Saline

NA: Numerical Aperture

CHAPTER 1

INTRODUCTION

1.1 Background

Leukemia, the cancer of blood cells, can be found in humans of all age groups. It is usually caused by the abnormal accumulation and proliferation of white blood cells. There are two types of leukemia, acute leukemia and chronic leukemia, classified based on the progress of blood cell accumulation. Comparatively speaking, chronic leukemia is more common in older people and develops much more slowly than acute leukemia.

B-cell Chronic Lymphocytic Leukemia (B-CLL) is one of the most common malignant lymphoid diseases in Western countries. B-CLL cells not only fail to generate any antibodies but accumulate in the bone marrow and occupy the space of healthy cells. Nowadays, B-CLL is described as a disease of accumulation, rather than proliferation, of monoclonal expensed B-lymphocytes in the blood, marrow, and lymphoid organs (Caligaris *et al.* 2007, Deaglio *et al.* 2003). CLL is an age-related, gender-related and familial disease. Most of CLL patients are over 50 years old, and the majority airmen. Moreover, people with a familial history are more likely to have CLL (Pekarsky *et al.* 2005). B-CLL is a disease could be either moderate or aggressive. Generally speaking, typical B-CLL is not a critical fatal leukemia; for typical B-CLL patients, the average survival time can be 25 years (Chiorazzi *et al.* 2010). However, B-CLL could also progress very aggressively in some cases, which are closely related to the poor-response of B-CLL treatments.

Such a difference in disease progression motivates researchers to improve diagnosis methods for poor-response B-CLL, and investigate its specific characteristics for prognostic. An ultimate goal is to assist physicians to develop more efficient and safer methods for the treatment of B-CLL.

1.2 Diagnosis of B-CLL

The typical diagnosis of B-CLL includes several procedures: firstly the total lymphocytosis concentration should be greater than 10^9/L of blood and the lymphocytes considered should be circulating mature-looking lymphocytes. Secondly, the expression of immunophenotypes on the cell surface is determined. The typical composition of immunological surface markers of B-CLL includes CD5+, CD19+, CD20+ etc., and a weak expression of monoclonal immunoglobulins (Caligaris *et al.* 2007). The term CD is the abbreviation for Cluster of Differentiation, which is coined for the surface marker (also called receptor or antigen) specially expressed on the membrane of white blood cells (Figure 1.1). The positive and negative sign refer to the positive expression and negative expression of the CD surface marker, respectively. B-CLL cells are only differentiated from B1 B-cells; and CD5 is expressed on lymphocytes such as B1 B-cells (Almasri *et al.* 1992). Therefore, CD5 is often used as an indicator of the B-CLL cell precursor. CD19 and CD20 are two immunophenotypes expressed on B-cells; the difference between those two is that the CD20 expression increases with the maturity of B-cells. Because B-CLL cells are usually immature B-cells, the expression of CD20 is weaker but still considered as a positive expression (Matutes *et al.* 2007).

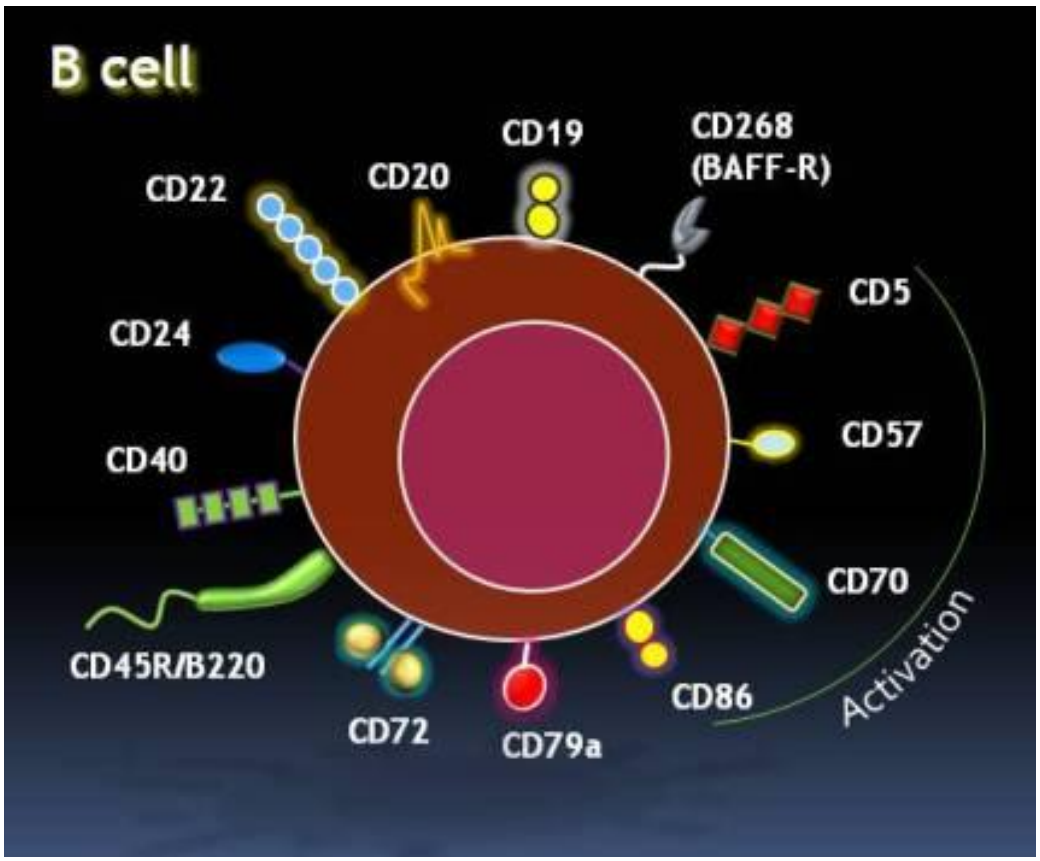

Figure 1.1: Different Cluster of Differentiation (CD) markers expressed on B-cell membranes. CD markers function as targets for specific antibodies, which provide immunophenotype information about the cell. *(Adapted from "A Drug for Chronic Fatigue Syndrome (ME/CFS)? The Rituximab Story, 2010.")*

Typical B-CLL cells originate from immature B-cells and usually have better clinical course and outcome (Pekarsky *et al.* 2005). Several parameters are associated with poor-response B-CLL, including lymphocyte doubling time (LDT) (>12 months), immunoglobulin variable region of heavy chain (IgV_H) gene mutations status, 13q del chromosomal abnormalities, telomere length, and impaired B cell receptor (BCR) signal transduction. For example, one of the poor-response B-CLL is derived from mature B-cells and corresponds to shorter LDT (<12 months), no IgV_H gene mutation status, 17p del or 11q del chromosomal abnormalities and intact

BCR signal transduction (Pekarsky *et al.* 2005). This group has much shorter survival time (< 8 years) and worse clinical outcome (Pekarsky *et al.* 2005, Chiorazzi *et al.* 2010). Interestingly one immunophenotype named as CD38, is always detected in this group. CD38 is believed to block B lymphopoiesis in bone marrow by decreasing the apoptosis signals of mature B-cells, which causes the abnormal proliferation of the mature B-cells (Hamblin *et al.* 2007). The positive expression of CD38 is correlated to the non-mutated IgV_H gene, which has been demonstrated as a surrogate marker of IgV_H gene status. But there is no evidence showing that the expression levels of CD38 and IgV_H gene status have a cause-and-effect relationship. The threshold to determine CD38+ B-CLL was set as 20% (Chiorzaai *et al.* 2005), or 30% (Hamblin *et al.* 2007) in different studies.

In addition to the presence of CD markers, the cell morphologies of different B-CLL cells differ (Chiorazzi *et al.* 2010). There are two commonly observed cell morphologies for B-CLL: typical and atypical cells. Typical B-CLL cells are small to medium in size (compared to the healthy cells), with clumped chromatin, an absent nucleolus and scanty cytoplasm; atypical B-CLL cells are larger with clumped chromatin, an absent or very small poorly defined nucleolus, and relatively abundant cytoplasm (Chiorazzi *et al.* 2010). Typical B-CLL patients contain very few atypical B-CLL cells while the poor-response B-CLL patients contain more than 15% of atypical B-CLL cells (Chiorazzi *et al.* 2010).

Clinically, fluorescent flow cytometry is the most commonly used technique to count the cell numbers with the presence of certain immunophenotypes. A fluorophore is attached to a specific antibody, which will bind only to the target cell surface marker expressed on the cells. The most commonly used fluorophores include Fluorescein Isothiocyanate (FITC), Cyanine 5 (Cy5), Phycoerythrin (PE), Phycoerythrin-Cyanine7 (PE-PC7) etc. The excitation and emission

wavelength data are shown in Appendix A as Figure A1. For instance, FITC-CD19 means that CD19 was bound to a fluorophore FITC labelled anti-CD19 antibody. The absence/presence of one immunophenotype is then determined based on fluorescence signals; cells are counted into negative/positive groups and the expression ratio of the immunophenotype is calculated based on cell counts. The flow cytometry results contain two axes, which stand for two distinct surface markers, such as PC7 labelled CD19 and PE labelled CD38 as shown in Figure 1.2A. Normally, the figure is divided into four areas, G1 (y-axis axis negative); and G4 (y-axis negative, x-axis positive). However, when the expression of immunophenotype is weak, or atypical cells are largely presented, flow cytometry yields obscure results, especially in the case of CD38 (Figure 1.2). The advantage of flow cytometry is that large numbers of cells are tested rapidly. But clinically used fluorescent flow cytometry lacks the direct observation of cell morphology and the positive expression distributions of surface markers on individual cells.

To achieve a better diagnosis and understanding of B-CLL, an alternative and complementary diagnosis method, fluorescence microscopy and image processing are introduced to directly visualize the cell morphology and quantitatively determine the level of immunophenotypes. The cell samples are illuminated with light of the specific wavelength according to the different fluorophore labels, which cause fluorescence in the samples. The corresponding emissions are detected through a microscope filter set and an objective. The images captured by a high-sensitivity camera are then processed with customized image processing software. For each wavelength, the cells showing positive signal will be counted, and the ratio of positive to negative cells determined for each surface marker of interest. Under a transparent (unfiltered) microscopy channel, which shows the morphology of the cells, the size, the cytoplasm area and other compartments of the cells can be clearly visualized and compared.

Those features significantly cover the defects of cytoplasm and supply a new path for the diagnosis and research of B-CLL.

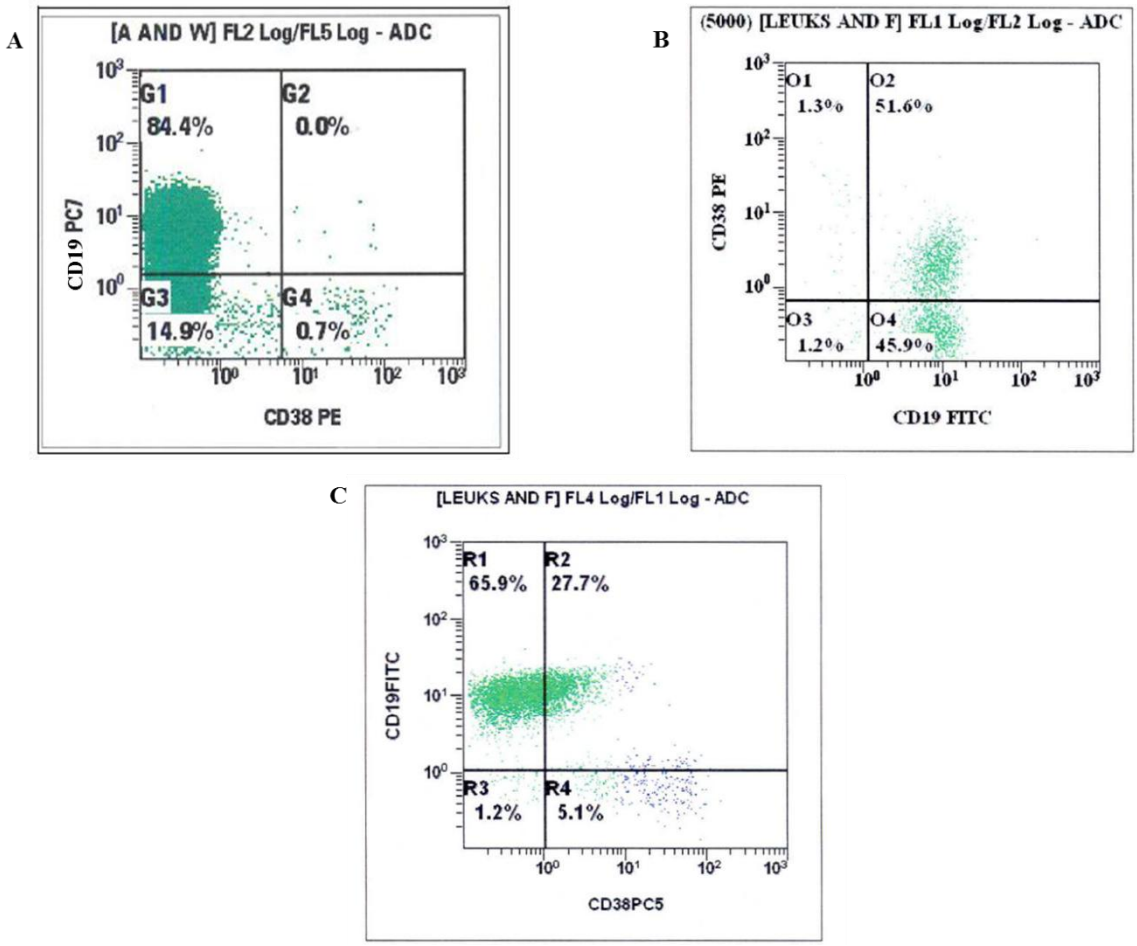

Figure 1.2: Fluorescence flow cytometry results: (A) CD38– sample (Patient IV); (B) CD38+ sample (Patient I); (C) obscure case (Patient II). The threshold used in the diagnosis is 30%. *(Results are provided by Dr. Chen Wang, Mount Sinai Hospital, Toronto)*

1.3 Thesis Objectives and Organisation

The primary objectives of this thesis are to determine the distribution of B-CLL surface markers, to supply a supplementary diagnosis of B-CLL, and to analyze the correlation between

surface marker and cell morphology. To achieve these goals, fluorophore-labeled antibodies were used to bind specific surface markers on the white blood cells and observed under specific microscopy channels (filter sets). A combined cell imaging and image processing method were developed to investigate the morphologies of the cells, and simultaneously obtain the expression status of surface markers. In order to further obtain a prognosis based on the expression of specific markers, *i.e.*, CD38, the expression correlation of CD38 with other surface markers, and the distribution patterns, have been quantitatively determined.

After a brief introduction of B-CLL in the first chapter of the thesis, the second chapter describes the proposed cell imaging technique, summarises the results obtained, and provides an analysis and discussion of the results. The work focussed on the morphology and size of leukemia cells, the expression correlation between CD38, CD5, CD19 and CD20, as well as their expression homogeneities on the cell surface. Another important investigation was to classify the B-CLL patients into CD38+ and CD38- categories.

The third chapter summarises the conclusions of this project, as well as the thesis contributions.

The Appendices describe the excitation and emission spectra of the fluorophores used in this work, and list the macro written for image processing, including the identification of the B-CLL cells and the analysis of the morphology parameters.

This project is multi disciplinary in nature, and as such involved three supervisors, Prof. Berini (optics/photonics) of the School of Electrical Engineering and Computer Science, and the Department of Physics; Dr. Shan Zou (chemistry), Measurement Science and Standards, National Research Council (NRC) Canada; and Dr. Chen Wang (medicine), Department of

Pathology and Laboratory Medicine, Mount Sinai Hospital, and Faculty of Medicine, University of Toronto. All imaging and data analysis work was carried out at the NRC under the supervision of Dr. Zou. The funding for this project was supplied by BiopSys NSERC Strategic Network for Bioplasmonic Systems.

1.4 References:

Caligaris-Cappio F, Ghia P. 2007. The normal counterpart to the chronic lymphocytic leukemia B cell. Best Pract Res Clin Haematol 20(3):385-97.

Deaglio S, Capobianco A, Bergui L, Durig J, Morabito F, Duhrsen U, Malavasi F. 2003. CD38 is a signalling molecule in B-cell chronic lymphocytic leukemia cells. Blood 102(6):2146-55.

Pekarsky Y, Calin GA, Aqeilan R, Croce CM. 2005. Chronic lymphocytic leukemia: Molecular genetics and animal models. Curr Top Microbiol Immunol 294:51-70.

Chiorazzi N, Damle RN, Wasil T. CD38 as a Prognostic Indicator in B-Cell Chronic Lymphocytic Leukemia. US Patent No.: US 7,842,461 B2., Nov. 30, 2010.

Almasri N, Duque R E, Iturraspe J, Everett E, Braylan R. 1992. Reduced expression of CD20 antigen as a characteristic marker for chronic lymphocytic leukemia. Am J Hematol 40:259-263.

Matutes E. 2007. Differential diagnosis in chronic lymphocytic leukaemia. Best Pract Res Clin Haematol 20(3):367-84.

Hamblin T. 2007. Prognostic markers in chronic lymphocytic leukemia. Best Pract Res Clin Haematol, 20(3): 455-468.

Chiorazzi N, Allen SL, Ferrarini M. 2005. Clinical and laboratory parameters that define clinically relevant B-CLL subgroups. Curr Top Microbiol Immunol 294:109-33.

CHAPTER 2:

Preamble: This chapter is presented in the form of a manuscript which has been recently published in the journal of *Microscopy Research and Technique 76:1147-1153* (2013), as well as some supplementary material included in sub-sections located thereafter. The manuscript describes the correlation between cell morphology and the expression of cell surface markers CD19, CD38, CD5 and CD20 on B-CLL cells. Furthermore, our cell counting technique gave a complementary diagnosis for patients whose flow cytometry results were too obscure to make any prognosis. All results were measured on patient samples by fluorescence microscopy and subsequent processing of captured images.

Author contributions: The sample preparation, cell imaging and image processing was carried out by Niu, including the implementation of computer codes needed for image processing and data analysis. Niu also produced the first draft of the manuscript and of the supplementary material. Chan provided a template from which the image processing code was developed. Niu, Berini, Zou and Wang contributed to the interpretation of the results. Berini, Zou and Wang edited the manuscript. The patient blood samples were prepared and supplied by Wang.

Morphology and Expression Status Investigations of Specific Surface Markers on B-cell Chronic Lymphocytic Leukemia (B-CLL) Cells

Suli Niu,[1,2] Ryan Chan,[1] Pierre Berini,[3] Chen Wang,[4] and Shan Zou[1*]

[1]*National Research Council Canada, 100 Sussex Drive, Ottawa, ON, K1A 0R6, Canada;*
[2]*Department of Chemical and Biological Engineering, University of Ottawa, 161 Louis Pasteur St., Ottawa, ON, K1N 6N5, Canada;*
[3]*School of Information Technology and Engineering, University of Ottawa, 161 Louis Pasteur Street, Ottawa, Ontario K1N 6N5, Canada; Department of Physics, University of Ottawa, 150 Louis Pasteur Street, Ottawa, Ontario, K1N 6N5, Canada*
[4]*Department of Pathology and Laboratory Medicine, Mount Sinai Hospital and Faculty of Medicine, University of Toronto, 600 University Avenue, Toronto, ON, M5X 1G5, Canada*

Keywords: B-cell Chronic Lymphocytic Leukemia, CD5, CD19, CD20, CD38, fluorescence microscope, Image J

Running title: Correlated cell morphology and surface marker expression

2.1 Abstract

The morphology of cells and expression status of specific surface markers (Cluster of Differentiation, CD), such as CD5, CD19, CD20, CD38 and CD45 have long been considered as the essential indicators for the diagnosis and prognosis of B-cell chronic lymphocytic leukemia (B-CLL). Clinically, it is difficult to simultaneously obtain cell morphology and distribution of surface markers with flow cytometry, especially for some surrogate markers such as CD38. Here, as an alternative and complementary prognostic method, fluorescence microscopy and image processing method are introduced to directly visualize the cells from patients and quantitatively determine the expression status of surface markers. In this study, the morphological parameters of B-CLL cells were measured, in order to establish the correlation between the cellular morphology and the surface marker expression. It was clear that the CD38+ and CD38– B-CLL cells from the same CD38+ patients had hardly any size differences, but an increase in perimeter was observed for CD38– patients. Moreover, the expression level of the receptors on the cell was independent of the cell size. There was no evidence showing that the expression intensities of CD19 and CD38 were related to each other for the CD38+ B-CLL cells. On the same cells, CD5 was more selectively expressed on the cell membrane; however, the expression patterns suggested that the cell membrane of CD38– B-CLL cells contained the least expression level of CD19.

2.2 Introduction

B-cell chronic lymphocytic leukemia (B-CLL) is identified as a disease that has both homogeneity and heterogeneity features (Caligaris-Cappio *et al.*, 2007; Chiorazzi*et al.*, 2005; Deaglio *et al.*, 2003). Its homogeneity is mainly reflected by its phenotype expression consistency (Caligaris-Cappio *et al.*, 2007; Deaglio *et al.*, 2003; Matutes, 2007). The heterogeneous aspect of B-CLL is associated with its clinical course variations: the progress of the B-CLL can be either indolent or aggressive (Caligaris-Cappio*et al.*, 2007; Deaglio *et al.*, 2003; Deaglio *et al.*, 2006). As previously introduced, the cellular morphology is one of the most important diagnostic factors for B-CLL. Matutes considered cellular morphology and surface marker expression status as two first-line laboratory investigations (Matutes, 2007). Several factors have been proved to have significant impacts on determination of subtype of B-CLL, which is essential both clinically and in leukemia research, including the gender, cellular morphology, bone marrow pattern, immunophenotype, chromosomal abnormalities, and IgV_H gene mutation status (Deterre *et al.*, 2000). Several reports had indicated that abnormal morphology was linked to the unmutated IgV_H region so as to positive expression of CD38; which is associated with a more aggressive case (Deaglio *et al.*, 2007; Reyes *et al.*, 1997). The threshold for the diagnosis of more aggressive B-CLL is the presence of more than 15% abnormal B-CLL cells (Matutes, 2007). Although there has been no direct evidence showing any causal nexus between CD38 expression level and the unmutated status of IgV_H gene, Deaglio *et al.* (Deaglio *et al.*, 2006) and others (Chu *et al.*, 2010) have suggested that the unmutated IgV_H gene associated to the positive CD38 expression (Chiorazzi *et al.*, 2010; Deaglio *et al.*, 2003), indicating CD38 can be a reliable prognostic marker for B-CLL patients. Hence, the

expression status of CD38 is one of the most important considerations of B-CLL for both clinical and research purposes (Hus *et al.*, 2006).

Fluorescent flow cytometry is the most commonly used technique in measuring B-CLL cell surface markers. To diagnose a patient as CD38+ B-CLL, at least 20% or 30% of total B-cells should be CD38+ (Deaglio *et al.*, 2006; Hamblin, 2003; Hus *et al.*, 2006). However, for some patients, the CD38 expression often presents as a continuous spectrum in its fluorescence intensity on flow cytometry graphs (see Figure 2.S1). Thus, it is difficult to have a clear cut-off between positive and negative expression levels using flow cytometry alone.

While flow cytometry analysis can provide phenotypic profile for the diagnosis of B-CLL, the heterogeneous cell morphology cannot be easily evaluated by conventional flow cytometry (Almasri *et al.*, 1992; Cabezudo *et al.*, 1999; Pekarsky *et al.*, 2005). Using fluorescence microscopy combined with automated data processing to image individual cells, the B-CLL cell morphology can be directly visualized and the characteristic expression status of surface markers can be simultaneously obtained. In this study, the expression status will be evaluated in three aspects: (1) the expression level of the surface markers, which can be calculated as the ratio of positive expressed cells to the total cells; (2) the expression intensity that can be determined by the fluorescence intensity, which reflects the amount of surface marker expressed on the cells; (3) the expression pattern of the surface marker that mirrors its expression position selectivity on the cell surface. Furthermore, the cell size distribution is found to be a morphological factor differentiating B-CLL cells. Similar to flow cytometry diagnosis, all above analyzes are determined based on fluorescence image analysis. The purpose of these investigations is to correlate cellular morphology, expression status and B-CLL types (less or more aggressive B-CLLs), in order to give complementary and improved prognosis of B-CLL.

2. 3 Methods

Sample Preparation

B-CLL cell samples were obtained from the samples used for diagnosis of the B-CLL patients in flow cytometry analyses at Mount Sinai Hospital, Toronto, ON. Briefly, the red blood cells were removed by using the lysing buffer (Beckman Coulter TQ Prep.). The B-CLL cells were enriched and suspended in 1% fetal calf serum (FCS) in PBS buffer (FCS buffer). Cells were re-suspended, and then 20 μL of fluorophore-labelled anti-surface marker antibodies (purchased from Beckman Coulter Inc. Canada) was added to the cell solution (see Section 2.8 for details).

Cell Imaging and Image Processing

All fluorescence and bright-field images were taken on an Olympus 1X81 fluorescence microscope equipped with a high sensitivity CCD camera (Cascade 512, Photometrics, US) and a 60X Plan Apochromat objective with the numerical aperture (NA) of 1.45. Depending on their absorbance characteristics, fluorophores were excited by lasers of appropriate wavelengths (488 nm Argon, 543 or 633 nm He-Ne lasers), and the emitted fluorescence was collected using filter sets with dichroic mirrors. More specific technical details and macro designs can be found in the Section 2.8. Briefly, customized macros in ImageJ were developed and used to efficiently locate cells on each captured fluorescence image and measure their sizes in perimeters, as well as to determine the fluorescence intensities of each surface marker on a given cell. For both macros, up to 2000 images can be loaded at the same time. Once the analysis of one image is finished,

the next uploaded image is opened and analyzed automatically. The final results including the long and short diameters, the intensity of the cell, and its quadrant intensities are summarized and saved as a text file for further analysis.

2.4 Results

Cellular Morphology Analysis

One of the most remarkable functions of image processing technique is the investigation of cell morphologies. Representative bright-field and fluorescence images of typical B-CLL cells are given in Figure 2.1. All cells present in a given area were imaged in bright-field mode, but cells visualized through a filter set were only those to which particular fluorophore-labelled antibodies were bound. Most of the B-CLL cells had a smooth round shape of diameter of 6-7 μm (Figure 2.1A). For this particular B-CLL sample, surface marker CD19 was bound with FITC-labelled anti-CD19 antibody (CD19-FITC) and CD38 was bound with PE labelled anti-CD38 antibody (CD38-PE). Figures 2.1B and 2.1C showed two representative epi-fluorescence images recorded using FITC filter set for CD19 and PE filter for CD38, respectively. All the cells visualized in Figure 2.1B were CD19 positive (CD19+) cells while the ones observed in Figure 2.1C were CD38 positive (CD38+) cells. The images shown in Figures 2.1B and 2.1C were taken from the same area of the same sample, which suggested that cells at the same position in each image were very likely the same ones. In Figures 2.1B and 2.1C, the cells co-expressing CD19 and CD38 were circled in yellow; they were termed CD19+/CD38+ cells whereas the cells expressing only CD19+ were termed CD19+/CD38– cells. The CD19+/CD38+ co-expression ratio was calculated by using the number of CD38+ B-CLL cells divided by

overall number of B-CLL cells. The co-expression ratio calculated for patients I-VII were 57.5%, 43.0%, 50.5%, 8.6%, 0.5%, 1.8% and 0.7%, respectively.

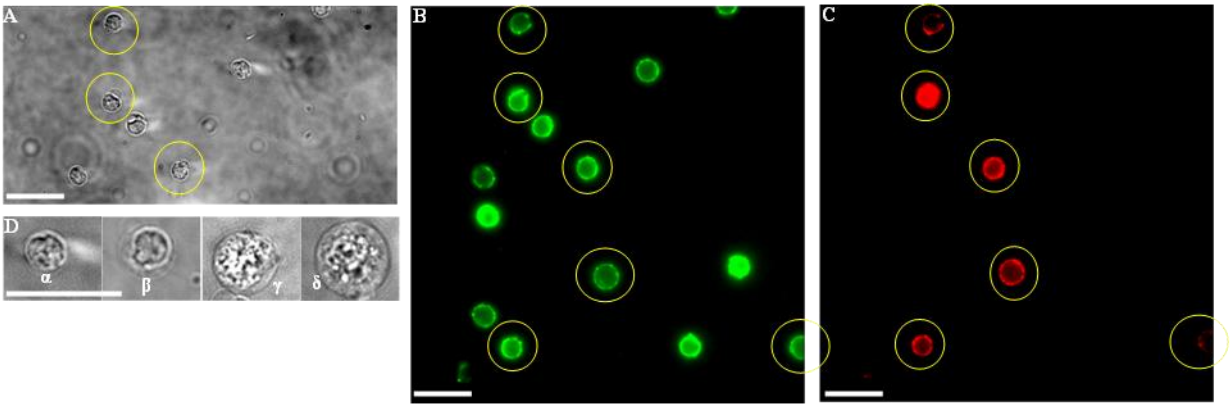

Figure 2.1: Bright-field and fluorescence images of white blood cells: bright-field images (A) and (D); fluorescence images of FITC-labelled CD19 (B); and PE-labelled CD38 (C). The cells present in images (B) and (C) were CD19+ and CD38+ cells from patient II, respectively. Cells co-expressing CD19 and CD38 appearing in both (B) and (C) were indicated in yellow circles. Cells α, β, γ and δ in (D) represent four types of morphologies observed: α represented the most common white blood cell morphology observed in CD38+ B-CLL samples; β represented swelled α cells; γ was the CD19–/CD38+ cell; and δ was CD19–/CD38– cell. The scale bars are 20 μm.

During image processing, we have found that the morphology and size of B-CLL cells were not identical for different patients, sometimes even different for the same patient. To give an example, Figure 2.1(D) showed four cell morphologies, representative of the four most frequently observed morphologies in our experiments. They were not necessary to be seen from the same patients. The morphology of labelled cell α was the most common CD19+/CD38+ and CD19+/CD38– cells present in the diagnosed CD38+ B-CLL patients, such as patient I, II and III. They had a large and condensed chromatin but a very small cytoplasm. In addition to uniform B-CLL cells, several larger cells or some elliptically-shaped cells were observed. The

cell labelled β in Figure 2.1D showed a case of B-CLL cell "swelling" where the nucleus was as large as that of a normal B-CLL cell and the cytoplasm area was enlarged significantly. In addition the boundary between the nucleus and the cytoplasm became clear. In Figure 2.1D, morphology γ showed the most common type of CD19–/CD38+ cells, and less than 1% of the cells had morphology δ shown in Figure 2.1D.

Another advantage of using an imaging technique is the ability to correlate cell morphologies with surface marker expression levels. Although the majority of B-CLL cells were roughly round in shape, B-CLL cells were better described as a bright elliptic ring on the epi-fluorescence images. We thus used the perimeter instead of the diameter as a size indicator. Typical cells were roughly composed of 5-pixel thick rings, and the perimeters were determined using the middle (3^{rd}) pixel rings. Firstly, the average perimeters of CD38+ B-CLL cells were measured on captured images using both CD19- and CD38-specific filter sets, respectively. Again, the CD38+ B-CLL cells were both CD19+ and CD38+. Due to the limited number of CD38+ B-CLL cells, patients IV, V, VI and VII were not included in this case, only cell samples from CD38+ B-CLL patients I, II and III were measured (Figure 2.2). It is worth noticing that the cell perimeters measured using different fluorescence labels and filter sets provided identical results for the same patient. In addition, for different patients, the variation of cell sizes is able to be identified. Specifically, patient I had the smallest perimeter (22.1 μm), which was 13% smaller than the perimeter of patient II, and 7% smaller than that of patient III.

Secondly, the sizes of CD38+ and CD38– B-CLL cells were investigated. The histograms of perimeters for CD38+ (left column) and CD38– (right column) B-CLL cells from all CD38+ patients I, II and III are shown in Figures 2.S3. Note that although the difference of the cell sizes measured using different filter sets for recording the images are negligible (Figure 2.2), to

minimize the influences, only size measurements obtained from images of CD19-FITC are compared. In consistent with the CD38+ results, the mean perimeter of CD38– B-CLL cells of patient I was the smallest. Interestingly, the average perimeters of CD38+ B-CLL cells were 2.3% and 3.3% larger than those of CD38– B-CLL cells for patients I and II, respectively (Figure 2.S3). On the contrary, for the patient III, the average perimeter of CD38+ B-CLL cells was 1.3% smaller (Figure 2.S3).

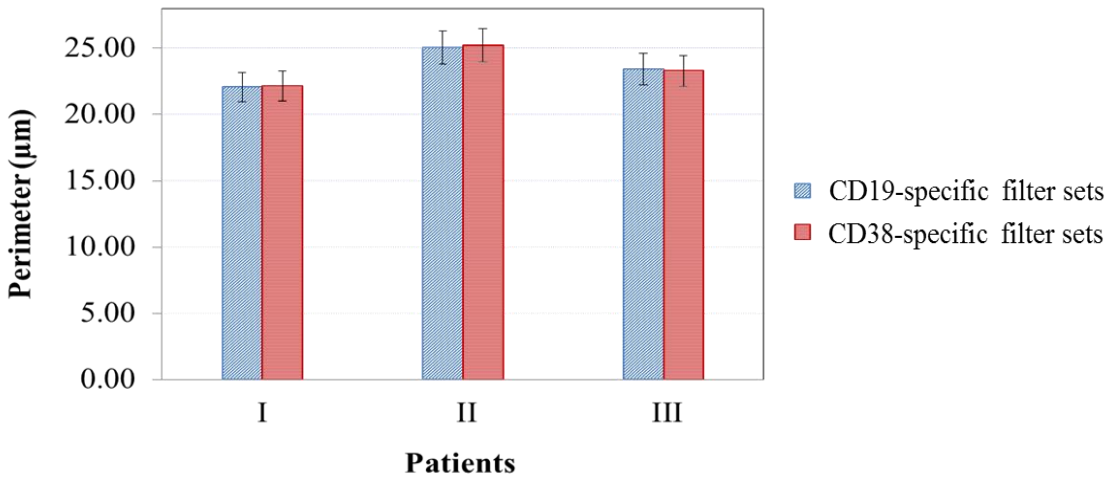

Figure 2.2: Perimeters of CD38+ B-CLL cells measured by using surface marker specific filter sets. The average perimeters of CD38+ B-CLL cells for each patient, captured using CD19-FITC filter set, were 22.1, 25.1 and 23.4 μm, respectively; the average perimeters of the same cell samples, measured in CD38-PE- or CD38-PC5-specific filter sets, were 22.2, 25.2 and 23.3 μm, respectively. An arbitrary error of ±5% was set by considering the uncertainty of 2 (±1) pixels in diameter determinations.

Thirdly, the sizes of B-CLL cells in CD38– B-CLL patients (IV-VII) were investigated (Figure 2.S4). The variation of the smallest average size to the largest one was as high as 16%, which was similar to the result obtained for CD38+ B-CLL patients. Notably, the perimeter distributions for individual patients IV, VI and VII were relatively large; and there were several "extremely" large cells present in the same sample.

Moreover, the data were summarized based on different B-CLL cell types, as shown in Figure 2.3. Firstly, for all three CD38+ patients, the perimeter difference of two sets of cells (CD38+ and CD38– cells) from the same patient were small, so it was safe to conclude that there was no appreciable size difference between CD38+ and CD38– B-CLL cells in the same CD38+ patient.

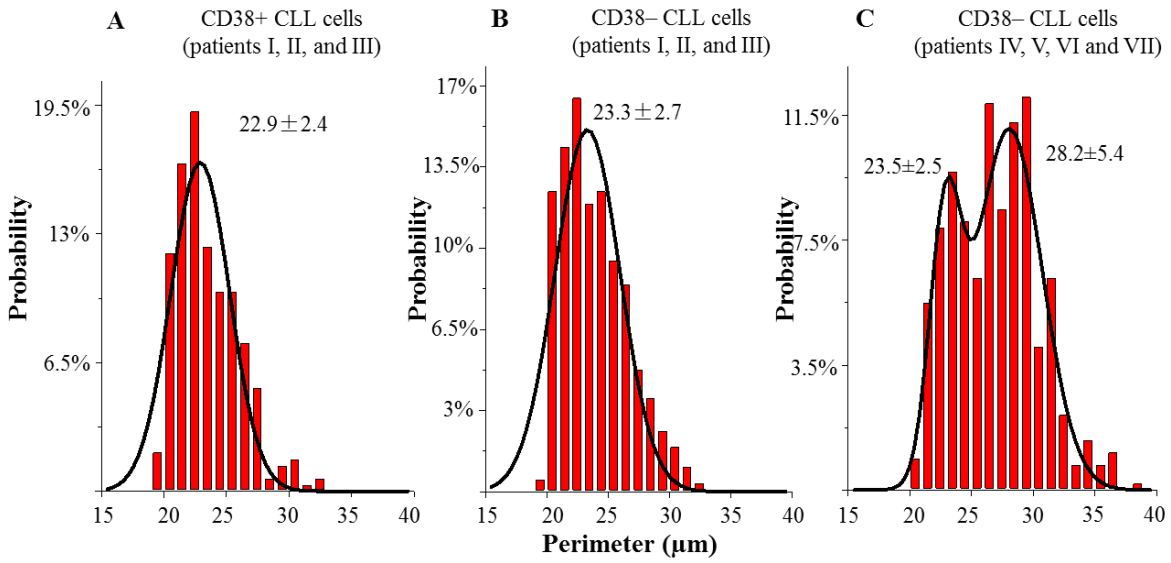

Figure 2.3: Histograms of perimeters of all CD38+ B-CLL cells from CD38+ patients (I-III) (A); all CD38– B-CLL cells from CD38+ patients (I-III) (B); and all CD38– B-CLL cells from CD38– patients(IV-VII) (C). The mean perimeters of CD38+ and CD38– B-CLL cells in CD38+ B-CLL patients were 22.9 μm and 23.3 μm, respectively, with narrow distributions. There were two fitted peaks (23.5 μm and 28.2 μm) for the mean perimeters of CD38– B-CLL cells from CD38– patients.

Secondly, the sizes of the same types of B-CLL cells were not preserved in different CD38+ B-CLL patients. Thirdly, the two populations of cell sizes found in patient V and VII might cause the two distribution peaks in Figure 2.3C. Additionally, the mean perimeter of CD38– B-CLL cells in CD38+ patients (23.3 μm) was generally smaller than those in CD38– patients (26.8 μm). As mentioned above, B-CLL, with better clinical outcome, has over 85% of

cells smaller than normal lymphocytes; and with worse clinical outcome has over 85% of cells larger than normal lymphocytes (Chiorazzi *et al.,* 2010). This is not consistent with our results, where the larger cells have been observed in better clinical outcome patient samples as well.

Fluorescence Intensity Analysis

Using imaging technique, we have analyzed the expression level of one specific surface marker, not only with regards to the number of cells expressing it, but also with regards to the amount of the surface marker on each cell. To analyze the expression status of surface markers, both the number of positively expressed cells and the amount of specific surface markers on each cell have been analyzed. First of all, there were several issues to be carefully considered. Most obviously, the emission intensities of different fluorophores labelled on antibodies were not directly comparable due to their diverse quantum efficiencies. Moreover, the status of florescence-labelled antibody, such as the number of fluorophore molecules per antibody or the binding ability and affinity to the surface markers, would certainly limit the direct comparisons of different fluorophores-labelled surface markers. Besides, the bleaching and quenching levels of different fluorophore labels may vary due to different excitation conditions, thus causing reduced fluorescence intensities with fluctuations. Taken all these factors into account as much as possible, we would only compare the surface markers labelled with the same fluorophores in different patients (such as CD19-FITC in patients I, II, and III) using the same excitation and similar emission conditions (sample substrates could not be the same) for imaging. The correlation between cell size and surface marker expression level was investigated by analyzing the relationship between perimeter and fluorescence intensity of each cell. An example was illustrated in Figure 2.4. For both surface markers CD19 and CD38, the perimeters and

intensities of the cells were nearly with no correlation to each other. The variation of fluorescence intensities indicated that the amounts of surface markers expressed on the cells varied, and this amount would not change with the increasing cell size.

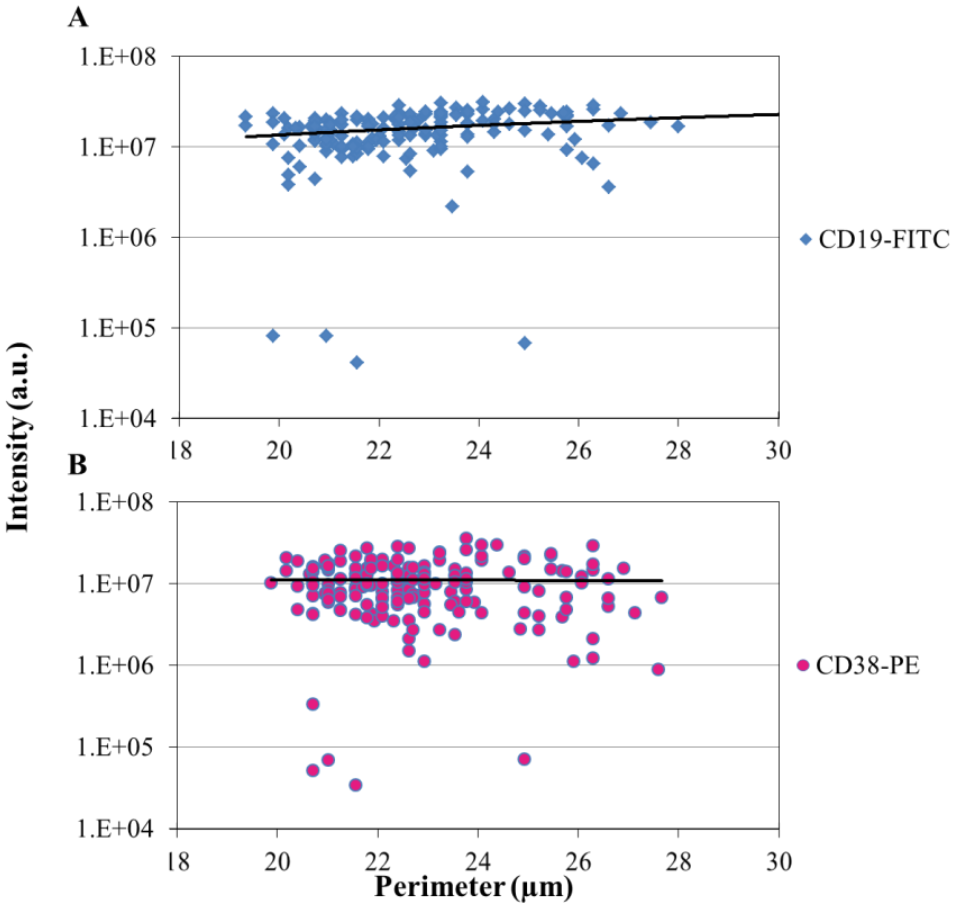

Figure 2.4: The correlation between expression intensity of surface markers and cell sizes. The measured 175 cells were all CD38+ B-CLL cells from patient I, CD19 was labelled by FITC (A) and CD38 was labelled by PE (B). Solid lines were linear fit to the data.

The intensity distributions of CD19-FITC and CD38-PE expressed on CD38+ B-CLL cells from CD38+ B-CLL patient I were measured on 175 cells and the results were summarized in Figure 2.5. The order was sorted with the ascending fluorescence intensities for CD19 in Figure

2.5A, and CD38 in Figure 2.5B. For majority of the cells, with increase of the CD19-FITC intensities, on the same CD38+ B-CLL cells, CD38-PE intensities were changing without any obvious associations; extremely high and extremely low readings exist in both cases. Meanwhile, for some of the cells (~30%), their CD19 intensities were found to be related to CD38 intensities.

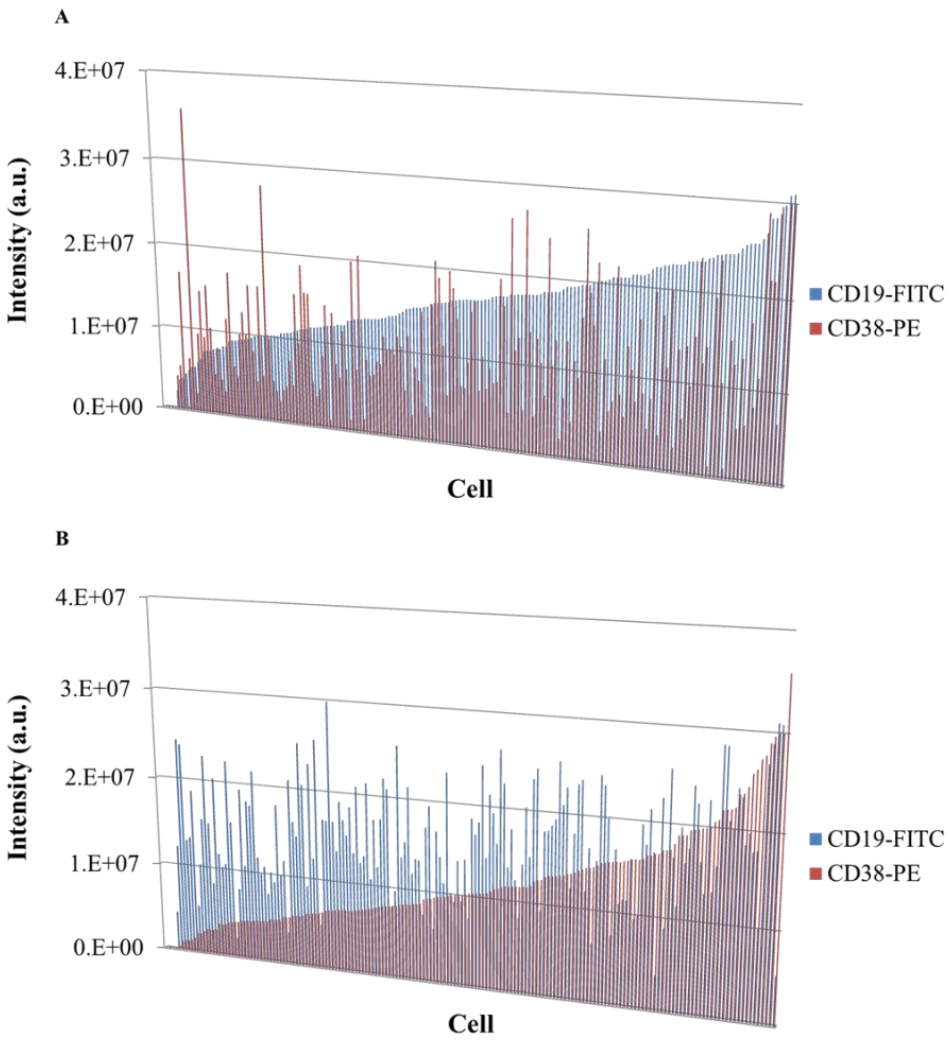

Figure 2.5: Fluorescence intensity correlation of CD19 and CD38 on CD38+ B-CLL cells of patient I. The intensities of CD19 were sorted with the ascending order (A); and for the same set of cells, the intensities of CD38 were sorted with the ascending order (B). The intensities of CD38 and CD19 were drawn accordingly. All the CD19 were labelled by FITC and the CD38 was labelled by PE.

The correlation of other surface markers such as CD5, CD19 and CD20 were important in the study of B-CLL (Almasri *et al.*, 1992; Ginaldi *et al.*, 1998; Insel*et al.*, 2010; Sheikh *et al.*, 2002). Two sets of comparisons were considered: one was between CD5-FITC and CD20-FITC in patients IV and VII, as illustrated in Figure 2.6A; the other was between CD19-PC7and CD20-PC7 in patients IV, V, VI and VII, as shown in Figure 2.6B.

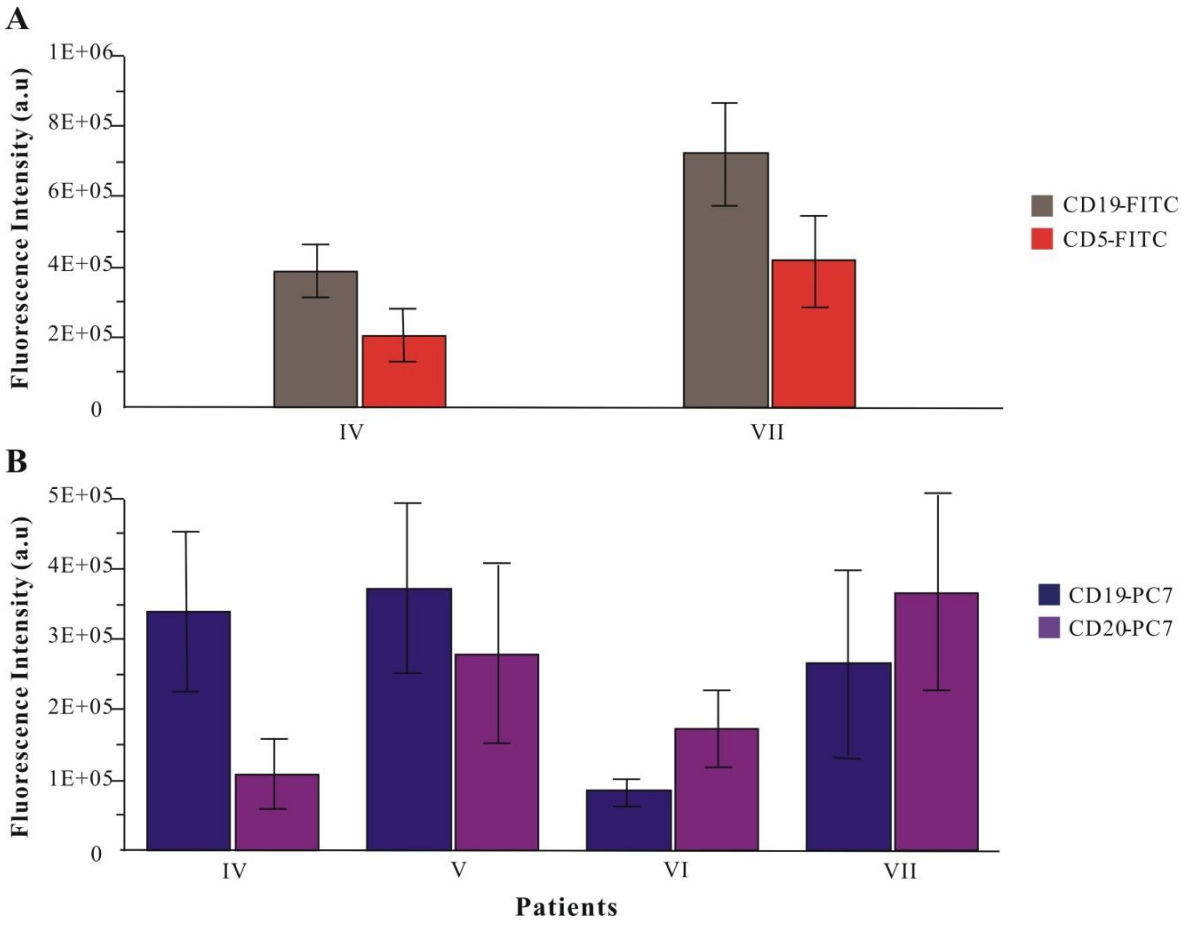

Figure 2.6: Fluorescence intensity of B-CLL cells from patient IV to VII. The fluorescence intensities comparisons of CD5-FITC and CD19-FITC (A), and CD19-PC7 and CD20-PC7 (B); the mean intensities and their standard deviation were obtained from the histograms fitted by Gaussian distribution.

In Figure 2.6A, within the same patient, the fluorescence intensities of CD19 were about 50% higher than those of CD5; for the same surface marker in two different patients, the intensities for patient VII were 100% larger than their intensities for patient IV. For the sets of CD19 and CD20, the intensities of CD19 were 60% and 20% higher than CD20 for patients IV and V, and 90% and 30% lower than CD20 for patients VI and VII, respectively (Figure 2.6B).

Surface Marker Distribution Patterns on CD38+ and CD38– B-CLL Cells

To investigate the surface marker distribution on B-CLL cells, each cell was divided into four quarters, and the fluorescence intensities of these four quadrants were measured. The quadrant intensity ratio was then calculated by using the fluorescence intensity of each quadrant divided by the sum of those four quadrants. This ratio represents the distribution evenness of specific surface markers. The standard deviations of calculated quadrant intensity ratios reveal the variation of the intensity ratios. When surface markers are evenly distributed on the cell surface, the average quadrant intensity ratio of each quarter should be 0.25. Smaller standard deviations indicate a more homogeneous distribution, and larger deviations indicate an increased heterogeneous distribution of surface markers on B-CLL cells. The quadrant intensity ratios from four groups of B-CLL cells were considered: (1) CD38+ cells measured using both CD19-FITC and CD19-PC7 filter sets, respectively; (2) CD38+ B-CLL cells measured with both CD38-PE and CD38-PC5 filter sets; (3) CD38– B-CLL cells from CD38+ patients using CD19-specific filter sets; and (4) CD38– B-CLL cells from CD38– patients using CD19-specific filter sets. It is worth noticing that the values measured using different filter sets can be combined in one histogram now. This is because the quadrant intensity ratio is an absolute value, which eliminates the error among different fluorophore-labels. The histograms associated with four sets of B-CLL

cells are shown in Figure 2.S5. The quadrant intensity ratios for all sets of cells involved in Figure 2.S5 were all around 0.25, and the corresponding standard deviations were 0.018, 0.022, 0.026 and 0.031, respectively.

Furthermore, quadrant intensity ratios of four surface markers on B-CLL cells were considered: CD5, CD19, CD20, and CD38. The corresponding histograms were shown in Figure 2.S6. Still, the mean ratios for all four surface markers were very close to 0.25, but the standard deviation various: CD5 had the largest standard deviation while CD19 and CD20 had the lowest standard deviations, with the value for CD38 in between.

2.5 Discussion

Fluorescence imaging has allowed us to directly visualize individual B-CLL cells with identified surface markers using specific labelled antibodies. The images taken from the same area of the same sample suggested that cells at the same position in each image were very likely the same cells. From the images, it is obvious that the fluorescence intensities of cells were not identical. Using the same filter set, some cells showed stronger intensity than others. Assuming the number of the same fluorescent labels is similar per antibody for all antibodies, the fluorescence intensity is then closely related to the expression status for the corresponding surface markers. Therefore the fluorescence intensity can be correlated to the expression amount of surface markers and the location of these labels on the cell membrane. Furthermore, using super-resolution techniques such as STED and STORM to obtain high-resolution images may provide direct insights into the expression level and correlation among surface markers.

The morphology and size of B-CLL cells were not identical even for the same patient; and the expression of surface markers could also correspond to the morphology and size variation of B-CLL cells. Two possibilities for the presence of large cells were cell swelling and a presence of different types of cells. The swelling of cells may happen when the concentration of cytosol inside the cell becomes larger and an osmotic pressure gradient is generated. The other types of larger cells were probably not B lymphocytes. Morphology γ showed the most common type of CD19– but CD38+ cell, which was most likely a T lymphocyte or a natural killer cell (Abousamra *et al.*, 2009). Morphology δ was CD19– and CD38–, and likely not lymphocytes but rather neutrophil cells.

The CD19+/CD38+ co-expression ratio can be utilized for the diagnosis of B-CLL and related to clinical outcome. For the samples in this study, CLL cells accounted for 90-99% of the

total B-cells based on flow cytometry results. Therefore, most CD19+ cells were CLL cells. In our microscopy studies, we have counted the CD19+ cells as a total number for comparison with other marker on B-CLL cells. Based on the diagnosis threshold of 30% for CD38+ expression ratio (Deaglio *et al.*, 2006), patients I, II and III were most likely to be CD38+ B-CLL patients, while patients IV, V, VI and VII were CD38– B-CLL patients. These conclusions were consistent with the flow cytometry results. In addition, for the obscure flow cytometry readings, such as the one for patient II, the co-expression ratio results obtained from cell imaging technique supply a complementary diagnosis for the physicians.

One type of fluorescence-labelled anti-surface marker antibody is believed to specifically target to corresponding surface marker and the fluorescence signals of a given cell are quantitatively detectable. Ideally, this fluorescence signal (intensity) should be proportional to the amount of corresponding surface markers on the cell membrane. Assuming the surface markers are homogeneously distributed on cell surfaces, the fluorescence intensity of a given surface markers should depend linearly on the cell size (or surface area). The variation of fluorescence intensities obtained in the measurements indicated that the amounts of surface markers expressed on the cells varied, and the flat slop between two parameters (Figure 2.4) indicated that the amount of the surface markers might be fixed for individual cells and would not be altered with the increasing of cell membrane area.

Most of the surface markers must collaborate with other markers, proteins, enzymes and lipids to complete cellular functions and processes. They are managed to participate in a variety of cell mechanisms by forming functional complex. Based on the assumptions, the intensities for CD19 and CD38 were assumed to be correlated to each other: the increase of CD19 or CD38 intensities were predicted to show an ascending order of CD38 or CD19 intensities, respectively.

However, only 30% of the results showed significant correlations between the expression of CD19 and CD38. The fluorescence intensity of CD19 was about 50% higher than that of CD5 on the same B-CLL cell (Figure 2.6A), indicating that for both patients IV and VII, the amount of CD19 markers was expressed more than CD5 on the B-cells. As for why there were more CD19+ cells than CD20+ cells (Figure 2.6B), it is well-known that at later stage of differentiation; the CD20 expression is down-regulated on these type B-lymphocytes while CD19 expression is up-regulated (Rawstron *et al.*, 2008, Ginaldi *et al.*, 1998).

In the cell images, it was obvious that some fluorescence labels were not evenly distributed on the cell surface, which suggested that the surface markers might be clustered and expressed heterogeneously on the cell surface. In most cases, on the same cell, the expression patterns of different surface markers were not identical, which meant that different surface markers could express on different positions on the membrane. Firstly, on the same set of B-CLL cells (*e.g.*, CD38+ cells), the expression of CD38 was more heterogeneous than the expression of CD19. Secondly, within the same type of patients (*i.e.*, CD38+ patients), CD19 expressed more homogeneously on CD38+ B-CLL cells than on CD38– B-CLL cells. Thirdly, on the same type of B-CLL cells, such as CD38– B-CLL cells, the CD19 expressed more heterogeneous on CD38– patients than on CD38+ patients.

Those standard deviations differences were most possibly caused by the surface markers distribution pattern. The homogeneity of the surface marker distribution revealed the expression preference on the cell membrane. A more heterogeneous distribution of a surface marker suggested that it expressed on specific cell membrane components selectively and sensitively. On CD38+ B-CLL cells, the CD38 was more selectively expressed on the cell membrane than CD19. The selectivity of CD19 was not identical in different B-CLL cell types and patient types.

Its expression on CD38– B-CLL cells from CD38– patients was found most sensitive on the cell membrane components. And the membrane components of CD38+ cells, as well as the CD38– B-CLL cells in CD38+ patients seemed to have less CD19 preferred compositions. Similarly, for the same set of cells, small standard deviations were found for CD19 and CD20 indicating a more homogeneous distributions. The larger deviation for CD5 indicates an increased heterogeneous distribution of CD5 on B-CLL cells. The restriction on the expression position of CD5 suggested that the CD5 was position-sensitive. It can only express on specific parts of the membranes. There was almost no difference on the expression of CD19 and CD20 for healthy B-cells, which indicates that the membrane positions they expressed were identical. For the CD38, it functions as a receptor for the Ca^{2+} level control once it interacts with CD19 on the lipid rafts parts of the cell membrane (Deaglio *et al.*, 2010), which explains why its express pattern was similar to that of CD19.

In summary, we have demonstrated that as an alternative and complementary prognostic method, fluorescence microscopy and automated data analysis are introduced to directly visualize cells from patients and quantitatively determine the expression status of surface markers. The expression status can be evaluated in three ways: (1) the expression level of the surface markers, which can be calculated as the ratio of positive expressed cells to the total cells; (2) the expression intensity that can be determined by the fluorescence intensity, which reflects the amount of surface marker expressed on the cells; (3) the expression pattern of the surface marker that mirrors its expression position selectivity on the cell surface. To correlate cellular morphology, expression status and B-CLL types, this imaging and processing method will provide new insights in the prognosis of B-CLL subtypes (Caligaris-Cappio, 1996; Deaglio *et al.*, 2006; Hamblin, 2007; Hus *et al.*, 2006; Shanafelt *et al.*, 2006).

2.6 Acknowledgement

The funding of this project is supplied by NSERC Strategic Network for Bioplasmonic Systems (BiopSys).

2.7 References

Abousamra NK, El-Din MS, Azmy E. 2009. T-cell CD38 expression in B-chronic lymphocytic leukaemia. Hematol Oncol 27(2):82-9.

Almasri NM, Duque RE, Iturraspe J, Everett E, Braylan RC. 1992. Reduced expression of CD20 antigen as a characteristic marker for chronic lymphocytic-leukemia. Am J Hematol 40(4):259-63.

Cabezudo E, Carrara P, Morilla R, Matutes E. 1999. Quantitative analysis of CD79b, CD5 and CD19 in mature B-cell lymphoproliferative disorders. Haematologica 84(5):413-8.

Caligaris-Cappio F. 1996. B-chronic lymphocytic leukemia: A malignancy of anti-self B cells. Blood 87(7):2615-20.

Caligaris-Cappio F, Ghia P. 2007. The normal counterpart to the chronic lymphocytic leukemia B cell. Best Pract Res Clin Haematol 20(3):385-97.

Chiorazzi N, Allen SL, Ferrarini M. 2005. Clinical and laboratory parameters that define clinically relevant B-CLL subgroups. Curr Top Microbiol Immunol 294:109-33.

Chiorazzi N, Damle RN, WasilT. 2010. CD38 as a prognostic indicator in B cell chronic lymphocytic leukemia. US Patent 7842461 B2.

Chu CC, Catera R, Zhang L, Didier S, Agagnina BM, Damle RN, Kaufman MS, Kolitz JE, Allen SL, Rai KR, Chiorazzi N. 2010. Many chronic lymphocytic leukemia antibodies recognize apoptotic cells with exposed nonmuscle myosin heavy chain IIA: implications for patient outcome and cell of origin. Blood 115(19):3907-15.

Deaglio S, Aydin S, Grand MM, Vaisitti T, Bergui L, D'Arena G, Chiorino G, Malavasi F. 2010. CD38/CD31 interactions activate genetic pathways leading to proliferation and migration in chronic lymphocytic leukemia cells. Mol Med 16(3-4):87-91.

Deaglio S, Capobianco A, Bergui L, Durig J, Morabito F, Duhrsen U, Malavasi F. 2003. CD38 is a signaling molecule in B-cell chronic lymphocytic leukemia cells. Blood 102(6):2146-55.

Deaglio S, Vaisitti T, Aydin S, Ferrero E, Malavasi F. 2006. In-tandem insight from basic science combined with clinical research: CD38 as both marker and key component of the pathogenetic network underlying chronic lymphocytic leukemia. Blood 108(4):1135-44.

Deaglio S, Vaisitti T, Billington R, Bergui L, Omede P, Genazzani AA, Malavasi F. 2007. CD38/CD19: a lipid raft-dependent signaling complex in human B cells. Blood 109(12):5390-8.

Deterre P, Berthelier V, Bauvois B, Dalloul A, Schuber F, Lund F. 2000. CD38 in T- and B-cell functions. Chem Immunol 75:146-68.

Ginaldi L, De Martinis M, Matutes E, Farahat N, Morilla R, Catovsky D. 1998. Levels of expression of CD19 and CD20 in chronic B cell leukaemia. J Clin Pathol 51(5):364-9.

Hamblin TJ. 2003. CD38: What is it there for? Blood 102(6):1939-40.

Hamblin TJ. 2007. Prognostic markers in chronic lympocytic leukaemia. Best Pract Res Clin Haematol 20(3):455-68.

Hus I, Podhorecka M, Bojarska-Junak A, Rolinski J, Schmitt M, Sieklucka M, Wasik-Szczepanek E, Dmoszynska A. 2006. The clinical significance of ZAP-70 and CD38 expression in B-cell chronic lymphocytic leukaemia. Ann Oncol 17(4):683-90.

Insel PA, Zhang L, Murray F, Kanter JR, Kipps T, Rassenti L. 2010. Diagnosis and treatment of chronic lymphocytic leukemia (CLL). US Patent 7846664 B2.

Matutes E. 2007. Differential diagnosis in chronic lymphocytic leukaemia. Best Pract Res Clin Haematol 20(3):367-84.

Pekarsky Y, Calin GA, Aqeilan R, Croce CM. 2005. Chronic lymphocytic leukemia: Molecular genetics and animal models. Curr Top Microbiol Immunol 294:51-70.

Rawstron AC, Hillmen P. 2008. Monoclonal B-cell lymphocytosis and chronic lymphocytic leukemia reply. New Engl J Med 359(19):2066.

Reyes E, Prieto A, Carrion F, Garcia-Suarez J, Esquivel F, Alvarez-Mon M. 1997. Morphological variants of leukemic cells in B chronic lymphocytic leukemia are associated with different T cell and NK cell abnormalities. Am J Hematol 55(4):175-82.

Shanafelt TD, Byrd JC, Call TG, Zent CS, Kay NE. 2006. Narrative review: Initial management of newly diagnosed, early-stage chronic lymphocytic leukemia. Ann Int Med 145(6):435-47.

Sheikh SS, Kallakury BVS, Al-Kuraya KA, Meck J, Hartmann DP, Bagg A. 2002. CD5-negative, CD10-negative small B-cell leukemia: Variant of chronic lymphocytic leukemia or a distinct entity? Am J Hematol 71(4):306-10.

2.8 Supplementary Information

Sample Preparation

The blood samples were processed with the standard lysing agent to remove the red blood cells. The B-CLL cells were collected and suspended in 1% fetal calf serum (FCS) in PBS buffer (FCS buffer). Cells were re-suspended, and then 20 μL of fluorophore-labelled anti-surface marker antibodies was added to the cell solution. The series labels and antibodies are listed in Table 2.S1 (*e.g.*, CD19-FITC referred to FITC labelled anti-CD19 antibody). The labelled sample solutions were vortexed every 5 min for 30-40 min. Then 1.4 mL FCS buffer was added to the solution and another centrifuge step (4000 rpm, 10 min) was conducted. Upon removing the supernatant solution, the pellet was re-suspended in 600 μL FCS buffer. The samples utilized in the experiments are listed in Table 2.S1.

Table 2.S2: Samples utilized in the experiments

Patient	Samples
J9201102 (I)	Sample 1: CD19-FITC, CD38-PE
J9140088 (II)	Sample 1: CD19-FITC, CD38-PE Sample 2: CD19-FITC, CD38-PC5
Jan 27 (III)	Sample 1: CD19-FITC, CD38-PC5
J6281801(IV)	Sample 1: CD38-PC5, CD19-PC7 Sample 2: CD19-FITC, CD38-PC5
J6071119 (V)	Sample 1: CD19-PC7 Sample 2: CD38-PC5
J5241011(VI)	Sample 1: CD19-FITC, CD38-PE Sample 2: CD19-PC7, CD38-PC5 Sample 3: CD38-PC5
J5101604(VII)	Sample 1: CD19-FITC Sample 2: CD19-PC7, CD38-PC5

15 μL of the labelled cell sample solution was spotted onto a cover slip (Fisher Scientific) covered with a perfusion chamber gasket (Invitrogen, Coverwell^{TM}, 20 mm diameter × 1.0 mm

deep). Prior to use, the glass cover slips were cleaned in piranha solution (3:1 H_2SO_4 (96%) : H_2O_2 (30%) by volume), then rinsed thoroughly with 450 mL Milli-Q water (18.3 MΩ cm) and dried in a nitrogen stream. ***Caution: Piranha solution should be handled with extreme caution; it has been reported to detonate unexpectedly***.

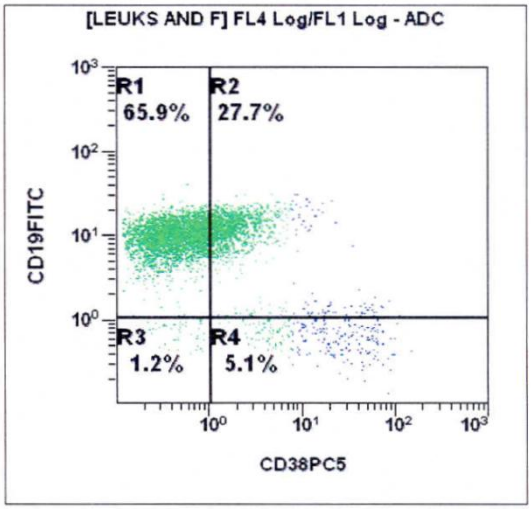

Figure 2.S1*: *An example of an unclear cut-off on a fluorescence intensity flow cytometry graph. The surface markers being tested were CD38-PC5 and CD19-FITC.

Cell Imaging and Data Processing. Specifically, the FITC and PC7 were excited by 488 nm Argon laser; and the PE and the PC5 were excited by 543 nm, and 633 nm HeNe lasers, respectively. One pixel is 0.267 µm wide and the full size of the images was 512×512 pixels. The cell counting and intensity values were measured in ImageJ with custom developed macros.

The fluorophore labelled antibodies bind specifically to the corresponding surface markers on the B-CLL cell surface. As expected, the captured fluorescence images were composed of dark background with bright rings that represent cells (Figure 2.S2).

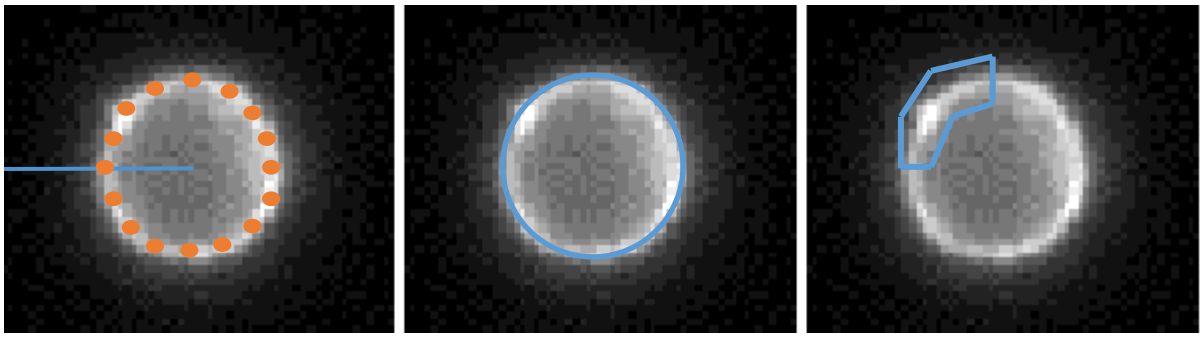

A B C

Figure 2.S2: An example showing the idea of cell detector macro (A), a diameter measurement (B), and quarter intensity polygon used for size measurements and intensity ratio calculation (C).

Customized macros (Macro 1 and 2) in ImageJ were developed and used to efficiently locate cells on each captured fluorescence image and measure their sizes in perimeters, as well as to determine the fluorescence intensities of each surface marker on a given cell.

To locate cells on a given image, the fluorescence intensities of all 512 by 512 pixels were first analyzed using Macro 1. The average fluorescence intensity of the darkest 200 pixels was set as the background intensity, and the standard deviation value of background ($S.D._{background}$) was calculated. Then, a line with 36 pixels in length was created and set to rotate 360 degree with its one end being the rotation centre. The line was set as 36 pixels long to ensure that a full B-CLL cell can be fully covered (the blue line in Figure 2.S2A). The line rotated from the pixel at the left top corner of the image, moved to the next pixel, and scan across the entire image. For each rotation, 16 moves that evenly distributed on the rotation circle with 22.5 degree angle were analyzed (the orange dots in Figure 2.S2A). For each of these 16 moves, the fluorescence intensities of 36 pixels were evaluated and a standard deviation ($S.D._{line}$) value was obtained. Again, for each full circle rotation, 16 standard deviation values were calculated. If 12 out of

these 16 $S.D._{line}$ values were larger than 3 times of the value of $S.D._{background}$, the center position of this rotation was recorded and one cell was counted.

A second macro (Macro 2) using the built-in "threshold" methods was generated to confirm and re-examine the location of the cell and to measure the size and fluorescence intensities of the cell. The mean intensity of the entire image was regarded as the background value in the built-in "threshold" methods. A binary image was generated with which the intensities of the pixels were larger than the background value being foreground. Those selected pixels could be individual or clustered pixels, representing free fluorophores or B-cells. To ensure that only B-cells were selected, a size verge of the pixel clusters was set between 30 pixels to 70 pixels, which matched the size range of a B-cell. If the pixel cluster size fell into this range, a cell was counted. And the position of the mass center of this cluster was determined and compared with the center obtained using Macro 1.

For each counted cell, an outer oval was drawn, which shared the centre and two diameters (long and short diameter) determined by the built-in "threshold" methods. An inner oval was then set using the same centre as the outer oval, with 14 pixels closer to the center. This is to ensure that all of the bright pixels representing the cell surface markers were enclosed between the two ovals. The diameters of the cell were determined by the program, and the perimeter of the cell was calculated by using the adjusted diameters (outer oval minus 7), the Figure 2.S2B showed the most common diameter size ring measured by the Macro 2. Each image was run by 17 different threshold methods and each of them returned a set of measurements. All results from different methods were compared with each other, and the cells with the most matched counts were selected as the final results and were used for next steps.

To obtain the relative intensity distribution (quadrant intensity ratio) of each cell, the image of an individual cell was processed using Macro 2. After a cell was detected, its centre and diameter were calculated. Then, two ovals were divided into four quarters with setting 12 points on both the outer and inner ovals, respectively. Those 12 points were evenly located on the ovals with 30° apart from each other. In each divided quarters, 8 points can be separately counted. A polygon was then drawn by connecting the 8 points anti-clockwise within each quarter. Figure 2.S2C clearly indicated the shape and position of one polygon. The fluorescence intensity of each pixel within the polygon was measured. The quadrant intensity ratio was calculated as the integrated intensity of a polygon divided by the total intensity of the cell, which equalled to the sum of the intensities of all four quadrants.

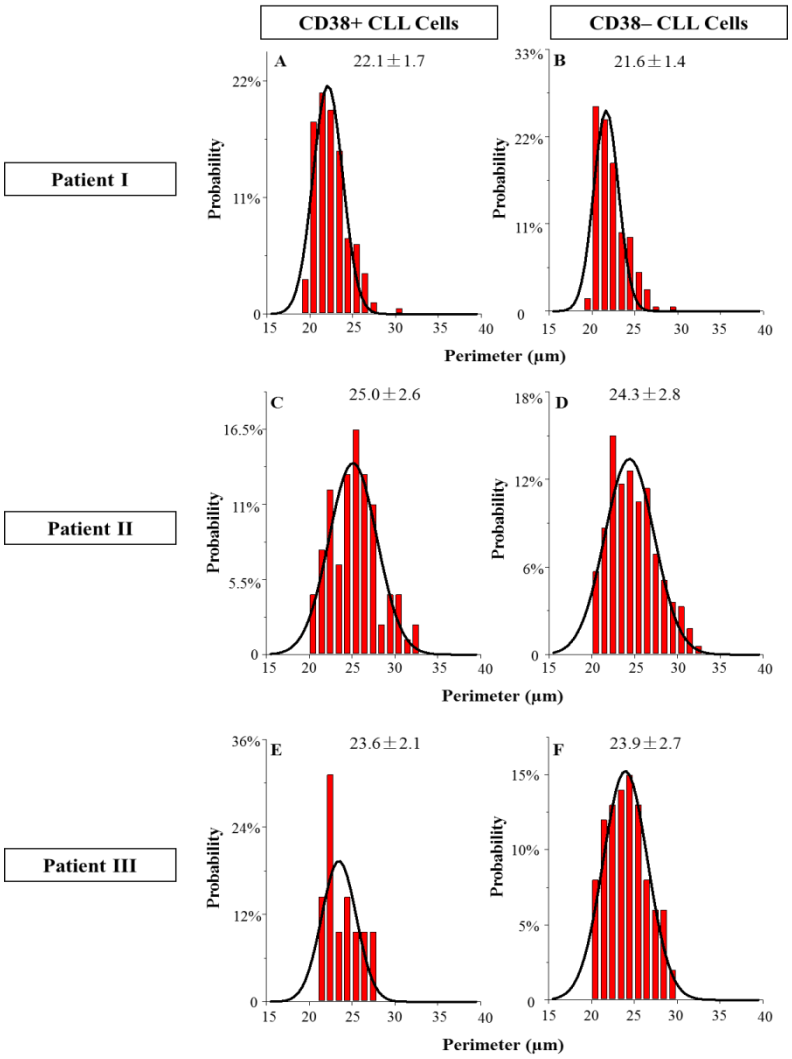

Figure 2.S3: The perimeter histograms of CD38+ (left) and CD38– (right) B-CLL cells for CD38+ B-CLL patients I (A and B), II (C and D) and III (E and F) were listed. The average perimeters were obtained by fitting the data to Gaussian and the mean values with their standard deviation are labelled in each plot.

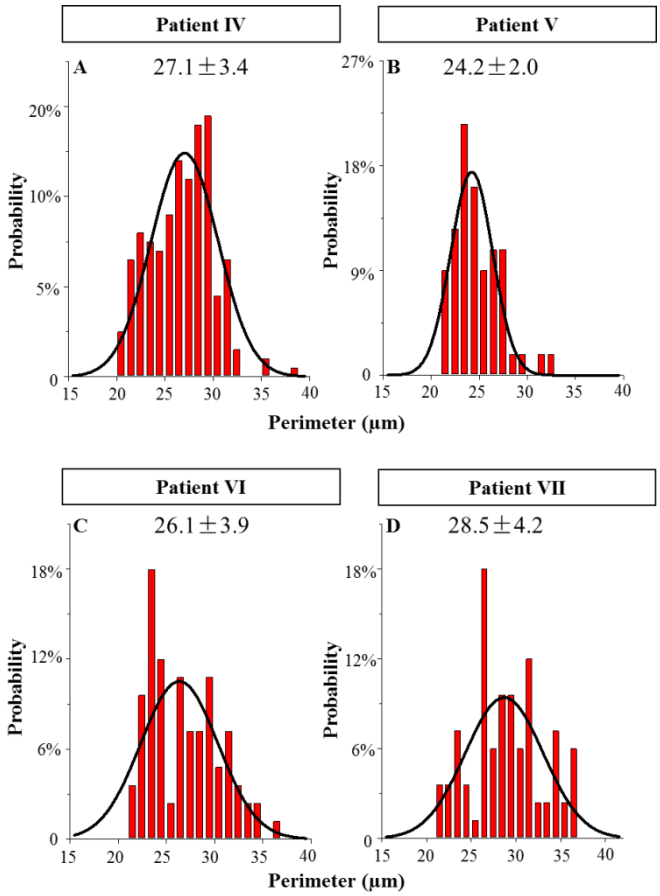

Figure 2.S4: The perimeter histograms of CD38– B-CLL cells for all CD38– patients IV (A), V (B), VI (C) and VII (D). The measurements were based on CD19-FITC specific images and the histograms were fit to Gaussian. The mean perimeters were 27.1, 24.2, 25.6 and 28.6 μm, respectively.

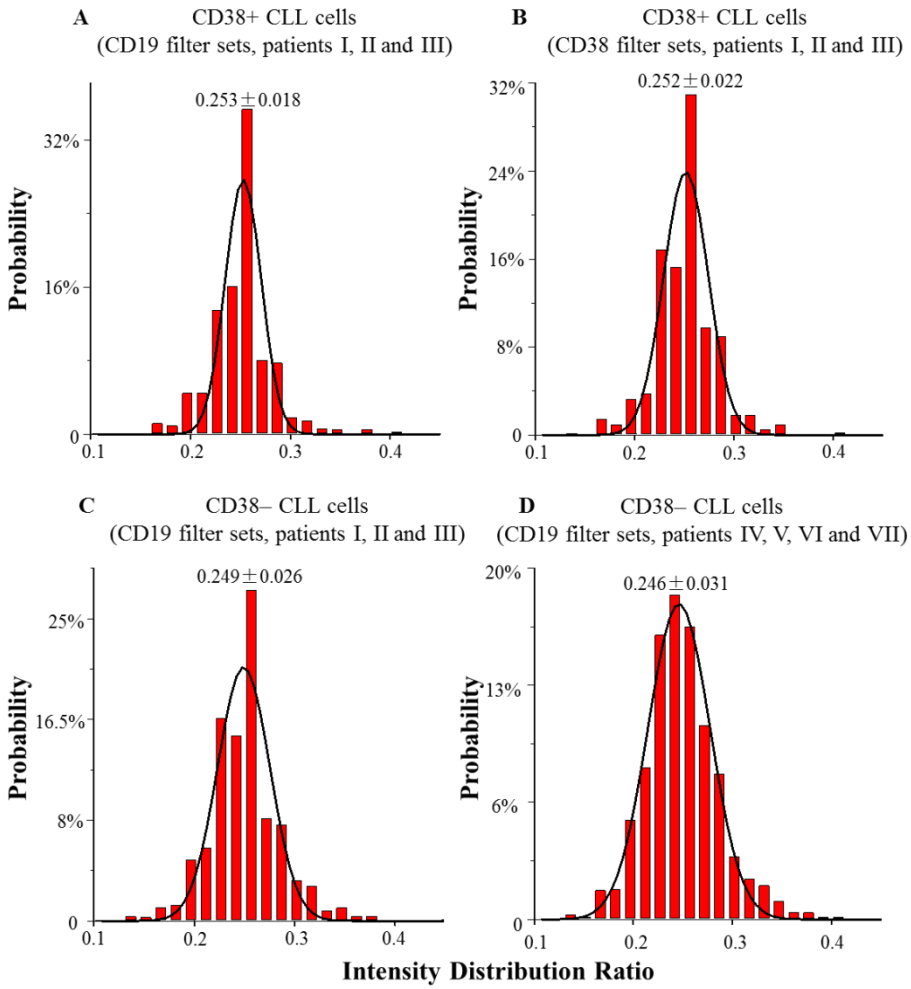

Figure 2.S5: Quadrant intensity ratio histograms for CD38+ B-CLL cells. Four different categories are summarized independently: quadrant intensity ratio distributions of CD38+ B-CLL cells with CD19-FITC (A); CD38+ B-CLL cells with CD38-PE and CD38-PC5 (B); CD38–B-CLL cells from CD38+ B-CLL patients (patient I, II and III) with CD19-FITC (C); CD38–B-CLL cells from CD38–B-CLL patients (patient IV, V, VI and VII) with CD19-FITC and CD19-PC7 (D).

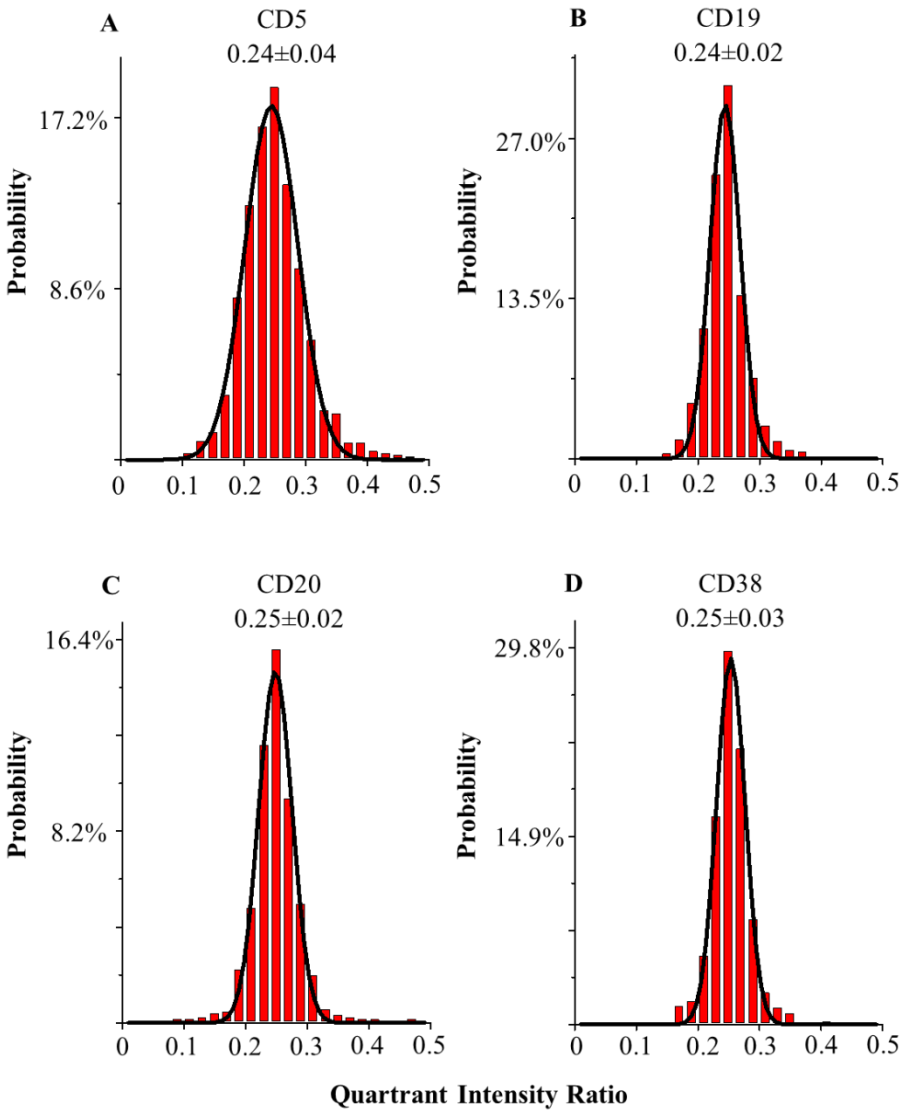

Figure 2.S6: Quadrant intensity ratio histograms for B-CLL cells. Four different surface markers were summarized independently: CD5 (A), CD19 (B), CD20 (C) and CD38 (D)

CHAPTER 3

CONCLUSIONS

A new method allowing the observation of cell morphology and the simultaneous analysis of surface marker expression on leukemia patient blood samples has been proposed and implemented. The method is based on the cell imaging and analysis of fluorophore-antibody-labelled B-CLL cell surface markers by fluorescence microscopy, which has provided a complementary diagnosis approach for patients with an obscure identification.

Imaging results clearly showed that the morphology and size of B-CLL cells were different from healthy ones, as were the surface marker distribution patterns. The former is due to the cell swelling phenomenon caused by the osmotic pressure gradient between the cytosol and environment; the latter is due to the position preference of surface markers. Relatively speaking, CD19 showed more homogenous expression on CD38+ B-CLL cells. Another correlation analysis was investigated between cell size and surface marker expression intensities and no obvious correlation was observed between them, which confirmed that the cell size enlarged mainly due to forces caused by an osmotic pressure gradient, thus not altering the amount of surface markers expressed thereon. However, on the same B-CLL cells, CD19 and CD38 always showed a positive correlation most possibly because they formed functional groups on the cell surface during Ca^{2+} transport.

A key outcome was the prognosis of the surrogate surface marker CD38 on B-CLL patients. After calculating the ratio of CD38+ B-CLL cells among all B-CLL cells, we could

conclude that patients I, II and III were CD38 positive (CD38+ B-CLL cells), suggesting that immediate treatment should be applied; patients IV, V, VI and VII were CD38 negative (CD38- B-CLL cells). Except for patient II, our results for all other patients were consistent with the tests based on flow cytometry, showing the validity of our newly developed method on the prognosis significance of CD38. Our imaging results also supplied a supplementary diagnosis for the case of patient II, whose boundary of CD38+ and CD38– obtained from flow cytometry was obscure. Cell morphology and image processing indeed provides an alternative and reliable way to diagnose B-CLL and obtain correlations between cell morphologies and (sub-) types of leukemia.

3.1 Future Work

Although this project supplied significantly more direct observation and analysis between cell size, morphology, surface marker expression correlation, and distribution pattern, more studies could be done by using the proposed technique. Firstly, in the diagnosis of CD38+ B-CLL, the ratio of CD38+ B-CLL cells was obtained by analysing hundreds of images. But some of the cells showed very weak positive CD38. By adopting a more accurate background subtraction method, which minimized the influence of the background signal on the intensity measurements, more accurate results could be generated and utilized to improve the diagnoses. Secondly, the research could be directed to determine the location of surface markers on the cell surface. Some surface markers expressed at the same position on the cell membranes might imply that they could form a complex during their participation in cell functions. Thirdly, the correlations were only considered between a group of two surface markers, *i.e.*, CD19 and CD38, CD19 and CD5. A more complex correlation, for instance, CD19 vs. CD20 vs. CD38 vs. CD5

could be calculated. Finally, in this research, we studied the surface marker expression by assuming the fluorescence intensity was linearly proportional to the amount of surface marker on the cell surface. If we could quantify the amount of fluorophores bound on the specific antibodies, we could calculate the exact number of surface marker expressed at different sample age (*e.g.*, with or without the treatments). This would bring a deeper understanding of surface marker expression on the B-CLL cells.

3.2 Publications:

- *Morphology and Expression Status Investigations of Specific Surface Markers on B-cell Chronic Lymphocytic Leukemia (B-CLL) Cells*

  Suli Niu, Ryan Chan, Pierre Berini, Chen Wang, and Shan Zou

  MICROSCOPY RESEARCH AND TECHNIQUE 76:1147–1153 (2013).

3.3 Presentations:

- 94th *Canadian Chemistry Conference* and Exhibition, June 2011, Montreal, QC.

  Oral Presentation: Quantitatively Determination of Surface Markers CD38 on B-cell Chronic Lymphocytic Leukemia Samples

- 93rd *Canadian Chemistry Conference* and Exhibition, June 2010, Toronto, ON.

  Poster presentation: Quantitatively Determination of CD38 Cell Surface Markers

- BiopSys All Network Meeting-3, January 2010, Toronto, ON.

Poster presentation(Best Poster Award): Quantitatively Determination of Surface Markers on B-CLL Cells

- BiopSys All Network Meeting-4, June 2010, Toronto, ON.

  Poster presentation: Quantitative Determination of CD20 and CD38 on B-CLL

- BiopSys All Network Meeting-5, January 2011, Toronto, ON.

  Poster presentation (Most Visually Effective Poster Award): Quantitative Determination of Cell Surface Markers on Chronic Lymphocytic Leukemia Patient Samples

Appendix A: Fluorescence Spectra of Fluorophores

A

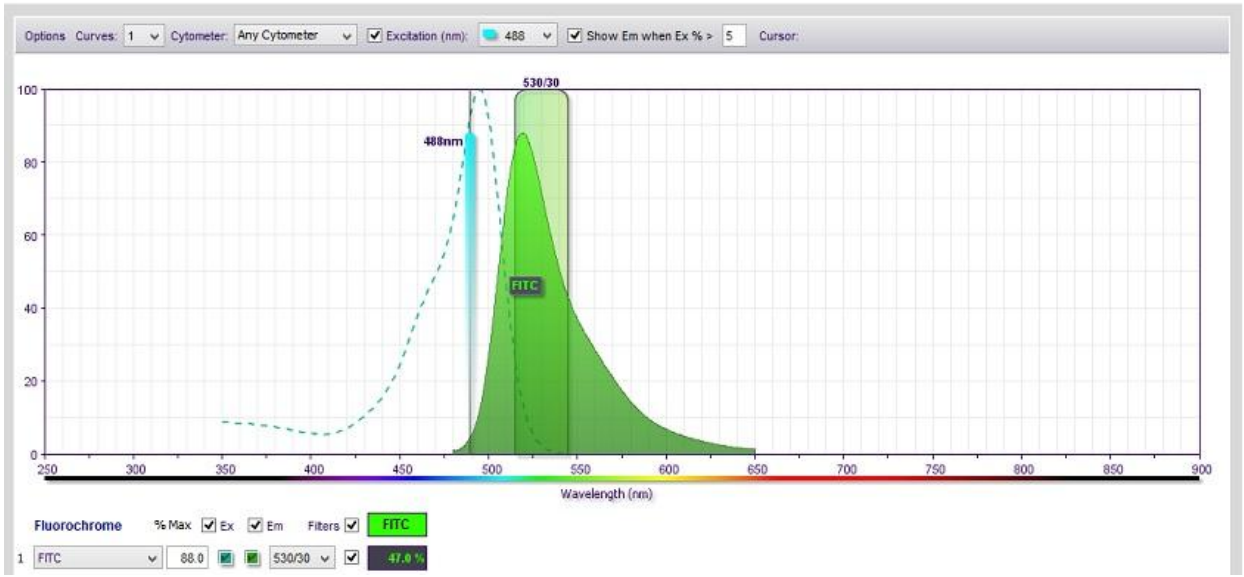

B

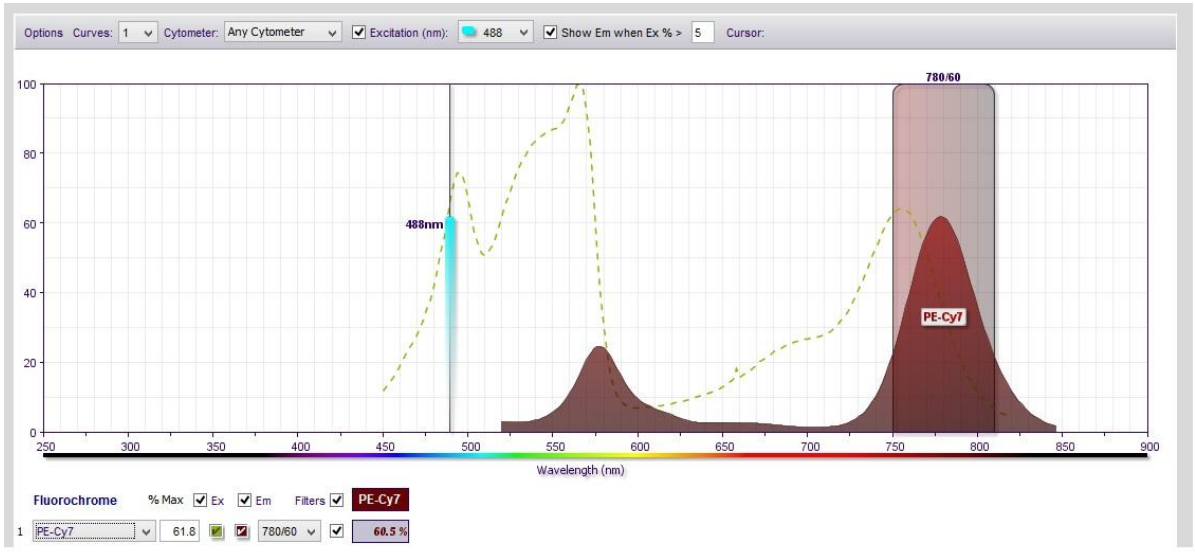

C

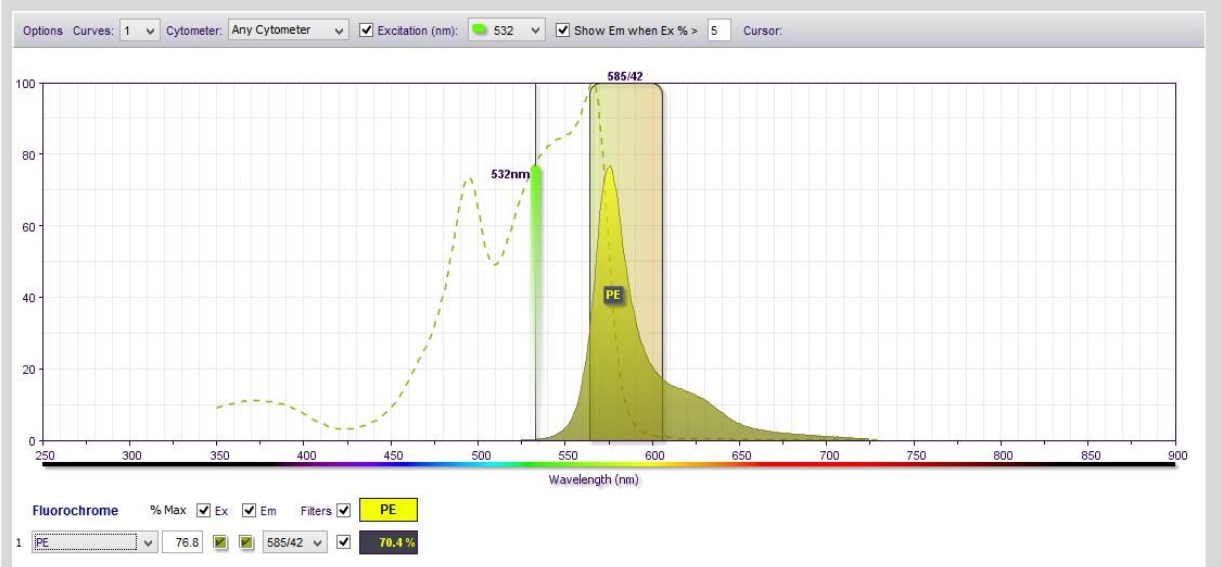

D

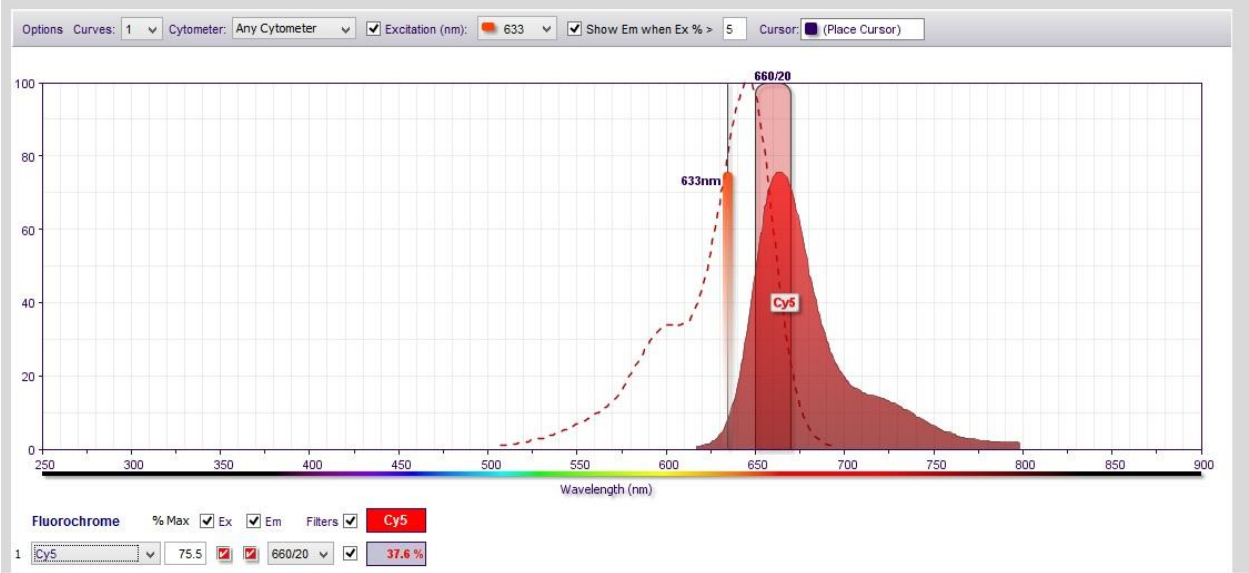

Figure A1: Fluorescence Spectra of FITC under 488 nm excitation wavelength (A), PC7 under 488 nm excitation wavelength (B), PE under 532 nm excitation wavelength (C), and Cy5 under 633 nm excitation wavelength (D). The dashed curves represent the excitation spectrum and the solid curves represent the emission. (The spectra were generated by *BD Fluorescence Spectrum Viewer*: *https://www.bdbiosciences.com/research/multicolor/spectrum_viewer/index.jsp)*

Appendix B: Image J code

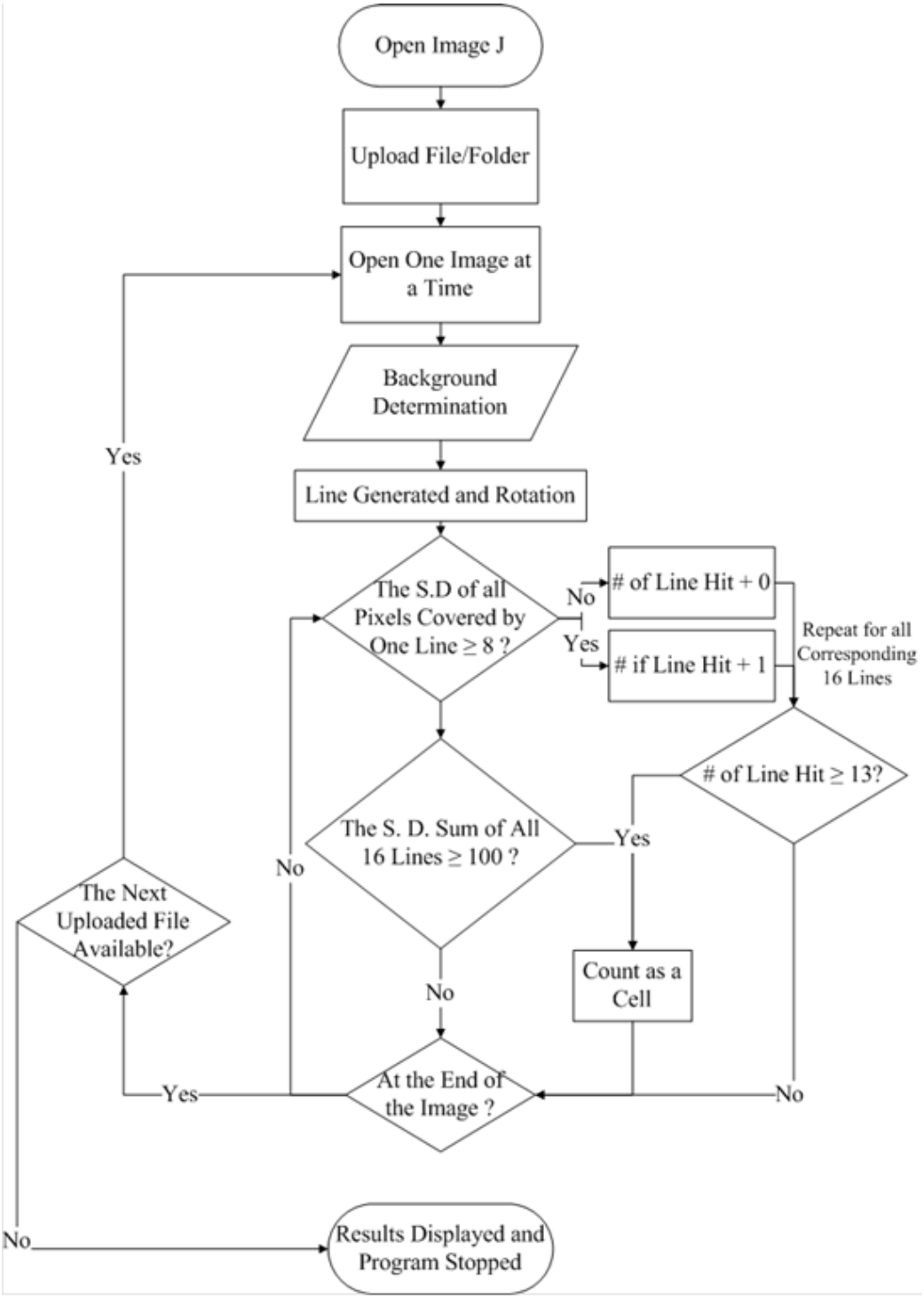

Figure B1: Description of cell detector macro process

Figure B2: Description of size and fluorescence intensity measurement macro process

```
//                          DECLARE VARIABLES

loop = 1;

var i = 0;

var paths = newArray( 20000 ); // It limited 20,000 images can be run at a same time. The threshold was set to 20000 to ensure enough space for images. The threshold was free to change depending on the number of images

var pathsid = newArray( 20000 );

var potcell = newArray( 20000 );

var pcpt=0;

var threshold;

var usethresholdmethod = newArray( 20 );

Array.fill(usethresholdmethod, true);

var backgroundthresholdmethod = "Mean"

var length = 30;

var maxlength =70;

var thicknessin = 7;

var thicknessout = 0; //The length, maxlength, thicknessin and thickness out were set depending on the true cell size (unit in pixels). To minimize fluorophore infect, the outside thickness of the cell ring was set to zero and inside ring thickness was set to 7. By substrate this thickness, the size of the cell in pixels could be calculated.

var intq;

var Perimeter;

var xx=3;

var yy=3;
```

```
var showallthresholds=true;

var logdet = 1;

var celltotal=0;

var closeimage = newArray(    "Never",

                    "After Each Image is Scanned",

                    "After all Images are Scanned" );

var ci = "After all Images are Scanned"; // Each image in the
chosen folder will be scanned one by one till the last image was
scanned.


var thresholdmethods = getList("threshold.methods");

usethresholdmethod[6] = true;


//                        MAIN MENU


do

{

     Dialog.create( "Shan - Menu" );

     items = newArray(   "Add Scan Files",

                    "Add Scan Folder",

                    "View/Delete Scan Files",

                    "Remove Scan File",

                    "Test/Change Threshold Type",

                    "Test/Change Background Threshold Type",

                    "Scan Files for Cells and Measure",

                    "Preferences",
```

```
                    "Access Other Windows",
                    "Quit" );
     Dialog.addChoice( "Action:", items );
     Dialog.show(); // There were ten functions were assigned
base on the analyze purpose.

     action = Dialog.getChoice();

     if( action == "Add Scan Files" )
          Add();
     else if( action == "Add Scan Folder" )
          AddFdr();
     else if( action == "View/Delete Scan Files")
          View();
     else if( action == "Remove Scan File")
          Remove();
     else if( action == "Test/Change Threshold Type")
          TTT();
     else if( action == "Test/Change Background Threshold Type")
          BTT();
     else if( action == "Scan Files for Cells and Measure" )
          NewCount();
     else if( action == "Preferences" )
          Preferences();
     else if( action == "Access Other Windows" )
          AOW();
```

```
     else
          loop=0;

}while(loop);

//                         FUNCTIONS

function Add()
{
     print( "Add Scan File in Operation" );
     paths[i] = File.openDialog( "Shan - Select Scan File #" +
(i+1) );
     print( paths[i], " successfully added" );
     i++;
     print( "" ); // This function allowed user to add single
image/file.
}

function AddFdr()
{
     print( "Add Scan Folder in Operation" );
     dir = getDirectory( "Select a folder containing all images
to be scanned" );
     list = getFileList(dir);
     print( "" );
     for( j=i; j<list.length+i; j++)
```

```
          paths[j]  =  dir+list[j-i];  //save  file  name  and
directory into path array


     // This function allowed user to add fold to the scan job
list. Each image in this fold will be saved into one position
and scanned.


     //delete all files that are not image files
     NotImg=0;


     for( q=0; q<j; q++ )
          if(  !endsWith(paths[q],  "")  &&  !endsWith(paths[q],
"gif" ))
          {
               for(qq=q; qq<j; qq++ )
                    paths[qq] = paths[qq+1];
               j--;
          }
     //display files added
     for( i; i<j; i++)
          print( paths[i], " successfully added" );
}


function View()
{
     print( "View Scan Files in Operation" );
```

```
for( q=0; q<i; q++ )
{
     print( "File #", q+1, ": ", paths[q] );
     open( paths[q] );
     pathsid[q]= getImageID();
     Cascade();
}

newImage( "DoNotCloseThisImage", "16-bit", 256, 1, 1 );
setLocation( 1400, 900 );
selectWindow( "DoNotCloseThisImage" );
close();

totaldeleted=0;
for( q=0; q<i; q++ )
{
     if( isOpen( pathsid[q] ) ){
          selectImage( pathsid[q] );
          close();
     }
     else{
          Delete(q-totaldeleted);
          totaldeleted++;
     }
}
```

```
     i-=totaldeleted;
     print( "" );
}

function Cascade()
{
     if( i<=3){
          if( q==0 )
               setLocation(0,0);
          if( q==1 )
               setLocation(  0.5*(screenWidth-512),  screenHeight-
492 );
          if( q==2 )
               setLocation( screenWidth-512, 0);
     }
     else if(i<=25){
          if( q%25<5)
               setLocation(q%5*275,0, 256, 256 );
          else if( q%25<10 )
               setLocation(q%5*275, 300, 256, 256 );
          else if( q%25<15 )
               setLocation(q%5*275, 600, 256, 256 );
          else if( q%25<20 )
               setLocation(q%5*275+90, 150, 256, 256 );
          else
               setLocation(q%5*275+90, 450, 256, 256 );
```

```
	}
	else{
		if(q%66<11)
			setLocation(q%11*130,0, 128, 128 );
		else if(q%66<22)
			setLocation(q%11*130,140, 128, 128 );
		else if(q%66<33)
			setLocation(q%11*130,280, 128, 128 );
		else if(q%66<44)
			setLocation(q%11*130,420, 128, 128 );
		else if(q%66<55)
			setLocation(q%11*130,560, 128, 128 );
		else
			setLocation(q%11*130,700, 128, 128 );
	}
}

function Remove()
{
	print( "Remove Scan File in Operation" );

	for( q=0; q<i; q++ )
		print( "File #", q+1, ": ", paths[q] );

	Dialog.create( "Shan - Delete Scan File" );
```

```
     Dialog.addNumber( "Select Scan File # to delete (zero to
return to main menu): ", 0 );
     Dialog.show();
     del = Dialog.getNumber();
     if(del==0)
          return;

     Delete(del-1);
     i--;

     print( "Background file successfuly deleted\n" );
}

function Delete(del)
{
     for( t=del; t<i; t++ )
          paths[t] = paths[t+1];
}
function TTT()
{
     methods = getList("threshold.methods");
     run( "Open..." );
     TTTpathid = getImageID();
     Tset=false;
     if( showallthresholds ){
          setLocation( 0,0,256,256 );
```

```
          for( z=0; z<methods.length; z++ ){
               run("Duplicate...", "title="+methods[z]);
                    if( z<5 ) setLocation(    (z+1)%6*240,    0,
256,256 );
                    else if (z<12) setLocation(   z%6*240,   300,
256,256 );
                    else if (z<18) setLocation(   z%6*240,   600,
256,256 );
                    setAutoThreshold(methods[z]+" dark");
          }
     }

     else setLocation( 125, 200, 512, 512 );

     do
     {
          if( !showallthresholds )
               setAutoThreshold(thresholdmethod+" dark");
          else
               Tset=true;


          Dialog.create( "Shan - Threshold Type" );
          Dialog.addChoice(   "Threshold   type:   ",   methods,
thresholdmethod);
          Dialog.addCheckbox( "Continue and Save", Tset );
          Dialog.show();
```

```
        thresholdmethod = Dialog.getChoice();
        Tset = Dialog.getCheckbox();
    }while( !Tset );

    selectImage( TTTpathid );
    run("Close");
    if( showallthresholds )
        for( z=0; z<methods.length; z++ ){
            selectWindow( methods[z] );
            run( "Close" );
        }

}// If there were some images in the chosen fold were unwanted,
the user can choose this option to delete them from the job
list.
function BTT()
{
    methods = getList("threshold.methods");
    run( "Open..." );
    TTTpathid = getImageID();
    Tset=false;
    if( showallthresholds ){
        setLocation( 0,0,256,256 );
        for( z=0; z<methods.length; z++ ){
            run("Duplicate...", "title="+methods[z]);
```

```
                    if( z<5 ) setLocation(    (z+1)%6*240,    0,
256,256 );
                    else if (z<12) setLocation(   z%6*240,   300,
256,256 );
                    else if (z<18) setLocation(   z%6*240,   600,
256,256 );
                    setAutoThreshold(methods[z]+" dark");
          }
     }

     else setLocation( 125, 200, 512, 512 );

     do
     {
          if( !showallthresholds )
               setAutoThreshold(thresholdmethod+" dark");
          else
               Tset=true;


          Dialog.create( "Shan - Threshold Type" );
          Dialog.addChoice(   "Threshold   type:   ",   methods,
backgroundthresholdmethod);
          Dialog.addCheckbox( "Continue and Save", Tset );
          Dialog.show();

          backgroundthresholdmethod = Dialog.getChoice();
```

```
          Tset = Dialog.getCheckbox();
     }while( !Tset );


     selectImage( TTTpathid );
     run("Close");
     if( showallthresholds )
          for( z=0; z<methods.length; z++ ){
               selectWindow( methods[z] );
               run( "Close" );
          }

}




function NewCount()
{
     run("Set Measurements...", "area mean standard min center
bounding redirect=None decimal=3");


     for( q=0; q<i; q++ )
     {
          xC = newArray( 2500 );
          yC = newArray( 2500 );
          hC = newArray( 2500 );
          wC = newArray( 2500 );
```

```
          vC = newArray( 2500 );

          tC = newArray( 2500 );

          nPC = newArray( 2500 );

          mC = newArray( 2500 );

          ICnPC = newArray( 2500 );

          ICmC = newArray( 2500 );

     bC = newArray( 2500 );

          pC=newArray(2500);

// Variety variables were set at maximum thresholds to ensure
enough space for data.

          open(paths[q]);

          pathsid[q]= getImageID();

          print( "Scanning ", paths[q], "..." );

          Background = FindBackground();

          //print(    "Background    Threshold    Method:\t    ",
backgroundthresholdmethod );

          //print( "Background Value: \t", Background );


          thresholdmethods = getList("threshold.methods");

          celltotal=0;

          for(   tm=0;   tm<thresholdmethods.length;   tm++   )if(
usethresholdmethod[tm] ){


               makeRectangle( 0,0,0,0 );

               //print(       "Threshold       Methods:       ",
thresholdmethods[tm] );

               setAutoThreshold(thresholdmethods[tm]+" dark");
```

```
for( r=0; r<nResults; r++ )
{
    if( getResult("Area",r)>0.785*length*length && getResult("Area",r)<0.785*maxlength*maxlength){//length check area
        makeOval(getResult( "XM", r )-0.5*getResult( "Width", r ), getResult( "YM", r )-0.5*getResult( "Height", r ), getResult( "Width", r ), getResult( "Height", r ));
        getRawStatistics( nPixels, mean, min, max, std, histogram );
        makeOval( getResult( "XM", r )-0.5*getResult( "Width", r )+thicknessin, getResult( "YM", r )-0.5*getResult( "Height", r )+thicknessin, getResult( "Width", r )-2*thicknessin, getResult( "Height", r )-2*thicknessin);
        getRawStatistics( ICnPixels, ICmean, ICmin, ICmax, ICstd, IChistogram );
        Value = nPixels*mean-ICnPixels*ICmean-Background*(nPixels-ICnPixels);
                                                    Ring = nPixels-ICnPixels;

        //save needed info here
        xC[celltotal] = getResult( "XM", r );
        yC[celltotal] = getResult( "YM", r );
        hC[celltotal] = getResult( "Height", r );
        wC[celltotal] = getResult( "Width", r );
```

```
                         vC[celltotal] = Value;
                         tC[celltotal] = thresholdmethods[tm];
                         nPC[celltotal] = nPixels;
                         mC[celltotal] = mean;
                         ICnPC[celltotal] = ICnPixels;
                         ICmC[celltotal] = ICmean;
                         bC[celltotal] =     Background;
;
pC[celltotal]=Ring;
                         celltotal++;
                    }
               }
          }

          for( qq=0; qq<celltotal; qq++ )
               for( s=0; s<(celltotal-1); s++ )
                    if( qq != s && xC[qq] <= xC[s]+0.5*length &&
xC[qq]  >=  xC[s]-0.5*length  &&  yC[qq]  <=  yC[s]+0.5*length  &&
yC[qq] >= yC[s]-0.5*length){
                         if( vC[qq] >= vC[s] )
                              vC[s]=0;
                         else
                              vC[qq]=0;
                    }

          for( qq=0; qq<celltotal; qq++ )
```

```
                if( vC[qq] == 0 ){
                     for( s=qq; s<(celltotal-1);s++){
                          xC[s] = xC[s+1];
                          yC[s] = yC[s+1];
                          hC[s] = hC[s+1];
                          wC[s] = wC[s+1];
                          vC[s] = vC[s+1];
                          tC[s] = tC[s+1];
                          nPC[s] = nPC[s+1];
                          mC[s] = mC[s+1];
                          ICnPC[s] = ICnPC[s+1];
                          ICmC[s] = ICmC[s+1];
                          bC[s] = bC[s+1];
pC[s]=pC[s+1];
                     }
                     celltotal--;
                     qq--;
                }
          //after analysis
          for( qq=0; qq<celltotal; qq++ ){
                     //print( "Cell #", qq+1, ":\t ", xC[qq], ",
",  yC[qq],  "\t",  vC[qq],  "\t",  tC[qq],  "\t",  wC[qq],  "\t",
hC[qq], "\t", (hC[qq]+wC[qq])/2-6);
                     //print( "Cell #", qq+1, ":\t ", vC[qq], " =
", nPC[qq], " * ", mC[qq], " - ", ICnPC[qq], " * ", ICmC[qq], "
- ", bC[qq], " * (", nPC[qq]," - ", ICnPC[qq], ")");
```

```
                    //makePolygon

     //1

makePolygon( xC[qq], yC[qq]-hC[qq]/2-1, xC[qq]-0.7*0.7*wC[qq]/2,
yC[qq]-hC[qq]/2+1,         xC[qq]-0.7*0.7*(wC[qq]/2-thicknessin),
yC[qq]-hC[qq]/2+thicknessin+1,          xC[qq],          yC[qq]-
hC[qq]/2+thicknessin);

getRawStatistics(q1nPixels,   q1mean,   q1min,   q1max,   q1std,
q1histogram);

        //print    (    xC[qq],    yC[qq]-hC[qq]/2-1,    xC[qq]-
0.7*0.7*wC[qq]/2,  yC[qq]-hC[qq]/2+1,  xC[qq]-0.7*0.7*(wC[qq]/2-
thicknessin),  yC[qq]-hC[qq]/2+thicknessin+1,  xC[qq],  yC[qq]-
hC[qq]/2+thicknessin);




        //2

makePolygon(xC[qq]-0.7*0.7*wC[qq]/2,  yC[qq]-hC[qq]/2+1,  xC[qq]-
0.35*wC[qq]-1,    yC[qq]-0.35*hC[qq]-1,    xC[qq]-0.70*(wC[qq]/2-
thicknessin),     yC[qq]-0.70*(hC[qq]/2-thicknessin),     xC[qq]-
0.7*0.7*(wC[qq]/2-thicknessin),                yC[qq]-(hC[qq]/2-
thicknessin)+1);

        //print(xC[qq]-0.7*0.7*wC[qq]/2,       yC[qq]-hC[qq]/2+1,
xC[qq]-0.35*wC[qq]-1,        yC[qq]-0.35*hC[qq]-1,        xC[qq]-
0.70*(wC[qq]/2-thicknessin),  yC[qq]-0.70*(hC[qq]/2-thicknessin),
xC[qq]-0.7*0.7*(wC[qq]/2-thicknessin),          yC[qq]-(hC[qq]/2-
thicknessin)+1);

getRawStatistics(q2nPixels,   q2mean,   q2min,   q2max,   q2std,
q2histogram);



       //3

makePolygon(xC[qq]-0.35*wC[qq]-1,    yC[qq]-0.35*hC[qq]-1,xC[qq]-
wC[qq]/2+1,       yC[qq]-0.7*0.7*hC[qq]/2,       xC[qq]-(wC[qq]/2-
thicknessin)+1,   yC[qq]-0.7*0.7*(hC[qq]/2-thicknessin),   xC[qq]-
```

```
0.70*(wC[qq]/2-thicknessin),                yC[qq]-0.70*(hC[qq]/2-
thicknessin));

getRawStatistics(q3nPixels,   q3mean,   q3min,   q3max,   q3std,
q3histogram);

        //print(xC[qq]-0.35*wC[qq]-1,         yC[qq]-0.35*hC[qq]-
1,xC[qq]-wC[qq]/2+1,  yC[qq]-0.7*0.7*hC[qq]/2,  xC[qq]-(wC[qq]/2-
thicknessin)+1,  yC[qq]-0.7*0.7*(hC[qq]/2-thicknessin),  xC[qq]-
0.70*(wC[qq]/2-thicknessin),                yC[qq]-0.70*(hC[qq]/2-
thicknessin));




        //4

makePolygon(xC[qq]-wC[qq]/2+1,  yC[qq]-0.7*0.7*hC[qq]/2,  xC[qq]-
wC[qq]/2-1,  yC[qq]+0.25,  xC[qq]-(wC[qq]/2-thicknessin),  yC[qq],
xC[qq]-(wC[qq]/2-thicknessin)+1,        yC[qq]-0.7*0.7*(hC[qq]/2-
thicknessin));

       //print(xC[qq]-wC[qq]/2+1,        yC[qq]-0.7*0.7*hC[qq]/2,
xC[qq]-wC[qq]/2-1,   yC[qq]+0.25,   xC[qq]-(wC[qq]/2-thicknessin),
yC[qq],          xC[qq]-(wC[qq]/2-thicknessin)+1,          yC[qq]-
0.7*0.7*(hC[qq]/2-thicknessin));

getRawStatistics(q4nPixels,   q4mean,   q4min,   q4max,   q4std,
q4histogram);




        //5

makePolygon(xC[qq]-wC[qq]/2+1,  yC[qq]+0.7*0.7*hC[qq]/2,  xC[qq]-
wC[qq]/2-1,  yC[qq]+0.25,  xC[qq]-(wC[qq]/2-thicknessin),  yC[qq],
xC[qq]-(wC[qq]/2-thicknessin)+1,        yC[qq]+0.7*0.7*(hC[qq]/2-
thicknessin));

getRawStatistics(q5nPixels,   q5mean,   q5min,   q5max,   q5std,
q5histogram);

        //print(xC[qq]-wC[qq]/2+1,       yC[qq]+0.7*0.7*hC[qq]/2,
xC[qq]-wC[qq]/2-1,   yC[qq]+0.25,   xC[qq]-(wC[qq]/2-thicknessin),
```

```
yC[qq],                          xC[qq]-(wC[qq]/2-thicknessin)+1,
yC[qq]+0.7*0.7*(hC[qq]/2-thicknessin));


       //6

makePolygon(xC[qq]-0.35*wC[qq]-1,    yC[qq]+0.35*hC[qq]+1,xC[qq]-
wC[qq]/2+1,       yC[qq]+0.7*0.7*hC[qq]/2,       xC[qq]-(wC[qq]/2-
thicknessin)+1,   yC[qq]+0.7*0.7*(hC[qq]/2-thicknessin),   xC[qq]-
0.70*(wC[qq]/2-thicknessin),              yC[qq]+0.70*(hC[qq]/2-
thicknessin));

getRawStatistics(q6nPixels,   q6mean,   q6min,   q6max,   q6std,
q6histogram);

       //print(xC[qq]-0.35*wC[qq]-1,
yC[qq]+0.35*hC[qq]+1,xC[qq]-wC[qq]/2+1,  yC[qq]+0.7*0.7*hC[qq]/2,
xC[qq]-(wC[qq]/2-thicknessin)+1,        yC[qq]+0.7*0.7*(hC[qq]/2-
thicknessin),                xC[qq]-0.70*(wC[qq]/2-thicknessin),
yC[qq]+0.70*(hC[qq]/2-thicknessin));


       //7

makePolygon(xC[qq]-0.7*0.7*wC[qq]/2,  yC[qq]+hC[qq]/2-1,  xC[qq]-
0.35*wC[qq]-1,    yC[qq]+0.35*hC[qq]+1,    xC[qq]-0.70*(wC[qq]/2-
thicknessin),     yC[qq]+0.70*(hC[qq]/2-thicknessin),     xC[qq]-
0.7*0.7*(wC[qq]/2-thicknessin),    yC[qq]+(hC[qq]/2-thicknessin)-
1);

getRawStatistics(q7nPixels,   q7mean,   q7min,   q7max,   q7std,
q7histogram);

        //print(xC[qq]-0.7*0.7*wC[qq]/2,       yC[qq]+hC[qq]/2-1,
xC[qq]-0.35*wC[qq]-1,        yC[qq]+0.35*hC[qq]+1,        xC[qq]-
0.70*(wC[qq]/2-thicknessin),  yC[qq]+0.70*(hC[qq]/2-thicknessin),
xC[qq]-0.7*0.7*(wC[qq]/2-thicknessin),          yC[qq]+(hC[qq]/2-
thicknessin)-1);


        //8
```

```
makePolygon( xC[qq], yC[qq]+hC[qq]/2+1, xC[qq]-0.7*0.7*wC[qq]/2,
yC[qq]+hC[qq]/2-1,         xC[qq]-0.7*0.7*(wC[qq]/2-thicknessin),
yC[qq]+hC[qq]/2-thicknessin-1,      xC[qq],      yC[qq]+hC[qq]/2-
thicknessin);

getRawStatistics(q8nPixels,   q8mean,   q8min,   q8max,   q8std,
q8histogram);

        //print(      xC[qq],      yC[qq]+hC[qq]/2+1,      xC[qq]-
0.7*0.7*wC[qq]/2,   yC[qq]+hC[qq]/2-1,   xC[qq]-0.7*0.7*(wC[qq]/2-
thicknessin),        yC[qq]+hC[qq]/2-thicknessin-1,        xC[qq],
yC[qq]+hC[qq]/2-thicknessin);



        //9

makePolygon(xC[qq],  yC[qq]+hC[qq]/2+1,  xC[qq]+0.7*0.7*wC[qq]/2,
yC[qq]+hC[qq]/2-1,         xC[qq]+0.7*0.7*(wC[qq]/2-thicknessin),
yC[qq]+hC[qq]/2-thicknessin-1,      xC[qq],      yC[qq]+hC[qq]/2-
thicknessin);

getRawStatistics(q9nPixels,   q9mean,   q9min,   q9max,   q9std,
q9histogram);

        //print(xC[qq],                         yC[qq]+hC[qq]/2+1,
xC[qq]+0.7*0.7*wC[qq]/2,                      yC[qq]+hC[qq]/2-1,
xC[qq]+0.7*0.7*(wC[qq]/2-thicknessin),          yC[qq]+hC[qq]/2-
thicknessin-1, xC[qq], yC[qq]+hC[qq]/2-thicknessin);



        //10

makePolygon(xC[qq]+0.7*0.7*wC[qq]/2,          yC[qq]+hC[qq]/2-1,
xC[qq]+0.35*wC[qq]+1,                      yC[qq]+0.35*hC[qq]+1,
xC[qq]+0.70*(wC[qq]/2-thicknessin),        yC[qq]+0.70*(hC[qq]/2-
thicknessin),              xC[qq]+0.7*0.7*(wC[qq]/2-thicknessin),
yC[qq]+(hC[qq]/2-thicknessin)-1);

        //print(xC[qq]+0.7*0.7*wC[qq]/2,       yC[qq]+hC[qq]/2-1,
xC[qq]+0.35*wC[qq]+1,                      yC[qq]+0.35*hC[qq]+1,
xC[qq]+0.70*(wC[qq]/2-thicknessin),        yC[qq]+0.70*(hC[qq]/2-
thicknessin),              xC[qq]+0.7*0.7*(wC[qq]/2-thicknessin),
yC[qq]+(hC[qq]/2-thicknessin)-1);
```

```
getRawStatistics(q10nPixels, q10mean, q10min, q10max, q10std,
q10histogram);



        //11

makePolygon(xC[qq]+0.35*wC[qq]+1,
yC[qq]+0.35*hC[qq]+1,xC[qq]+wC[qq]/2-1,  yC[qq]+0.7*0.7*hC[qq]/2,
xC[qq]+(wC[qq]/2-thicknessin)-1,        yC[qq]+0.7*0.7*(hC[qq]/2-
thicknessin),                 xC[qq]+0.70*(wC[qq]/2-thicknessin),
yC[qq]+0.70*(hC[qq]/2-thicknessin));

getRawStatistics(q11nPixels, q11mean, q11min, q11max, q11std,
q11histogram);

       //print(xC[qq]+0.35*wC[qq]+1,
yC[qq]+0.35*hC[qq]+1,xC[qq]+wC[qq]/2-1,  yC[qq]+0.7*0.7*hC[qq]/2,
xC[qq]+(wC[qq]/2-thicknessin)-1,        yC[qq]+0.7*0.7*(hC[qq]/2-
thicknessin),                 xC[qq]+0.70*(wC[qq]/2-thicknessin),
yC[qq]+0.70*(hC[qq]/2-thicknessin));



        //12

makePolygon(xC[qq]+wC[qq]/2-1,          yC[qq]+0.7*0.7*hC[qq]/2,
xC[qq]+wC[qq]/2+1,  yC[qq]+0.25,  xC[qq]+(wC[qq]/2-thicknessin),
yC[qq],                         xC[qq]+(wC[qq]/2-thicknessin)-1,
yC[qq]+0.7*0.7*(hC[qq]/2-thicknessin));

getRawStatistics(q12nPixels, q12mean, q12min, q12max, q12std,
q12histogram);

       //print(xC[qq]+wC[qq]/2-1,        yC[qq]+0.7*0.7*hC[qq]/2,
xC[qq]+wC[qq]/2+1,  yC[qq]+0.25,  xC[qq]+(wC[qq]/2-thicknessin),
yC[qq],                         xC[qq]+(wC[qq]/2-thicknessin)-1,
yC[qq]+0.7*0.7*(hC[qq]/2-thicknessin));



        //13
```

```
makePolygon(xC[qq]+wC[qq]/2-1,          yC[qq]-0.7*0.7*hC[qq]/2,
xC[qq]+wC[qq]/2+1,  yC[qq]+0.25,  xC[qq]+(wC[qq]/2-thicknessin),
yC[qq],         xC[qq]+(wC[qq]/2-thicknessin)-1,         yC[qq]-
0.7*0.7*(hC[qq]/2-thicknessin));

getRawStatistics(q13nPixels,  q13mean,  q13min,  q13max,  q13std,
q13histogram);

      //print(xC[qq]+wC[qq]/2-1,        yC[qq]-0.7*0.7*hC[qq]/2,
xC[qq]+wC[qq]/2+1,  yC[qq]+0.25,  xC[qq]+(wC[qq]/2-thicknessin),
yC[qq],         xC[qq]+(wC[qq]/2-thicknessin)-1,         yC[qq]-
0.7*0.7*(hC[qq]/2-thicknessin));



      //14

makePolygon(xC[qq]+0.35*wC[qq]+1,            yC[qq]-0.35*hC[qq]-
1,xC[qq]+wC[qq]/2-1,  yC[qq]-0.7*0.7*hC[qq]/2,  xC[qq]+(wC[qq]/2-
thicknessin)-1,           yC[qq]-0.7*0.7*(hC[qq]/2-thicknessin),
xC[qq]+0.70*(wC[qq]/2-thicknessin),        yC[qq]-0.70*(hC[qq]/2-
thicknessin));

      //print(xC[qq]+0.35*wC[qq]+1,          yC[qq]-0.35*hC[qq]-
1,xC[qq]+wC[qq]/2-1,  yC[qq]-0.7*0.7*hC[qq]/2,  xC[qq]+(wC[qq]/2-
thicknessin)-1,           yC[qq]-0.7*0.7*(hC[qq]/2-thicknessin),
xC[qq]+0.70*(wC[qq]/2-thicknessin),        yC[qq]-0.70*(hC[qq]/2-
thicknessin));

getRawStatistics(q14nPixels,  q14mean,  q14min,  q14max,  q14std,
q14histogram);



       //15

makePolygon(xC[qq]+0.7*0.7*wC[qq]/2,           yC[qq]-hC[qq]/2+1,
xC[qq]+0.35*wC[qq]+1,                       yC[qq]-0.35*hC[qq]-1,
xC[qq]+0.70*(wC[qq]/2-thicknessin),        yC[qq]-0.70*(hC[qq]/2-
thicknessin),   xC[qq]+0.7*0.7*(wC[qq]/2-thicknessin),   yC[qq]-
(hC[qq]/2-thicknessin)+1);

getRawStatistics(q15nPixels,  q15mean,  q15min,  q15max,  q15std,
q15histogram);
```

```
        //print(xC[qq]+0.7*0.7*wC[qq]/2,       yC[qq]-hC[qq]/2+1,
xC[qq]+0.35*wC[qq]+1,                        yC[qq]-0.35*hC[qq]-1,
xC[qq]+0.70*(wC[qq]/2-thicknessin),        yC[qq]-0.70*(hC[qq]/2-
thicknessin),    xC[qq]+0.7*0.7*(wC[qq]/2-thicknessin),    yC[qq]-
(hC[qq]/2-thicknessin)+1);


        //16

makePolygon(xC[qq],  yC[qq]-hC[qq]/2-1,  xC[qq]+0.7*0.7*wC[qq]/2,
yC[qq]-hC[qq]/2+1,         xC[qq]+0.7*0.7*(wC[qq]/2-thicknessin),
yC[qq]-hC[qq]/2+thicknessin+1,          xC[qq],          yC[qq]-
hC[qq]/2+thicknessin);

       //print(xC[qq],                          yC[qq]-hC[qq]/2-1,
xC[qq]+0.7*0.7*wC[qq]/2,                       yC[qq]-hC[qq]/2+1,
xC[qq]+0.7*0.7*(wC[qq]/2-thicknessin),                    yC[qq]-
hC[qq]/2+thicknessin+1, xC[qq], yC[qq]-hC[qq]/2+thicknessin);

getRawStatistics(q16nPixels,  q16mean,  q16min,  q16max,  q16std,
q16histogram);




 //point 1

makePoint(xC[qq], yC[qq]-hC[qq]/2-1);

getRawStatistics(qP1nPixels, qP1mean);

        //print(qP1nPixels, ",", qP1mean);


//point 2

makePoint(xC[qq], yC[qq]-hC[qq]/2+thicknessin);

getRawStatistics(qP2nPixels, qP2mean);

        //print(qP2nPixels, ",", qP2mean);
```

```
//point 3
makePoint(xC[qq]-0.7*0.7*wC[qq]/2, yC[qq]-hC[qq]/2+1);
getRawStatistics(qP3nPixels, qP3mean);
        //print(qP3nPixels, ",", qP3mean);


//point 4
makePoint(     xC[qq]-0.7*0.7*(wC[qq]/2-thicknessin),     yC[qq]-
(hC[qq]/2-thicknessin)+1);
getRawStatistics(qP4nPixels, qP4mean);
        //print(qP4nPixels, ",", qP4mean);

//point 5
makePoint(xC[qq]-0.35*wC[qq]-1, yC[qq]-0.35*hC[qq]-1);
getRawStatistics(qP5nPixels, qP5mean);
        //print(qP5nPixels, ",", qP5mean);

//point 6
makePoint(xC[qq]-0.70*(wC[qq]/2-thicknessin),yC[qq]-
0.70*(hC[qq]/2-thicknessin));
getRawStatistics(qP6nPixels, qP6mean);
        //print(qP6nPixels, ",", qP6mean);


//point 7
makePoint(xC[qq]-wC[qq]/2+1, yC[qq]-0.7*0.7*hC[qq]/2);
```

```
getRawStatistics(qP7nPixels, qP7mean);
        //print(qP7nPixels, ",", qP7mean);

//point 8
makePoint(xC[qq]-(wC[qq]/2-thicknessin)+1,                yC[qq]-
0.7*0.7*(hC[qq]/2-thicknessin));
getRawStatistics(qP8nPixels, qP8mean);
        //print(qP8nPixels, ",", qP8mean);

//point 9
makePoint(xC[qq]-wC[qq]/2-1, yC[qq]+0.25 );
getRawStatistics(qP9nPixels, qP9mean);
        //print(qP9nPixels, ",", qP9mean);

//point 10
makePoint(xC[qq]-(wC[qq]/2-thicknessin), yC[qq]);
getRawStatistics(qP10nPixels, qP10mean);
        //print(qP10nPixels, ",", qP10mean);

//point 11
makePoint(xC[qq]-wC[qq]/2+1, yC[qq]+0.7*0.7*hC[qq]/2);
getRawStatistics(qP11nPixels, qP11mean);
        //print(qP11nPixels, ",", qP11mean);

//point 12
```

```
makePoint(xC[qq]-(wC[qq]/2-thicknessin)+1,
yC[qq]+0.7*0.7*(hC[qq]/2-thicknessin));

getRawStatistics(qP12nPixels, qP12mean);

        //print(qP12nPixels, ",", qP12mean);


//point 13

makePoint(xC[qq]-0.35*wC[qq]-1, yC[qq]+0.35*hC[qq]+1);

getRawStatistics(qP13nPixels, qP13mean);

        //print(qP13nPixels, ",", qP13mean);


//point 14

makePoint(xC[qq]-0.70*(wC[qq]/2-thicknessin),
yC[qq]+0.70*(hC[qq]/2-thicknessin));

getRawStatistics(qP14nPixels, qP14mean);

        //print(qP14nPixels, ",", qP14mean);


//point 15

makePoint(xC[qq]-0.7*0.7*wC[qq]/2, yC[qq]+hC[qq]/2-1);

getRawStatistics(qP15nPixels, qP15mean);

        //print(qP15nPixels, ",", qP15mean);


//point 16

makePoint(xC[qq]-0.7*0.7*(wC[qq]/2-thicknessin),
yC[qq]+hC[qq]/2-thicknessin-1);

getRawStatistics(qP16nPixels, qP16mean);

        //print(qP16nPixels, ",", qP16mean);
```

```
//point 17
makePoint(xC[qq], yC[qq]+hC[qq]/2+1);
getRawStatistics(qP17nPixels, qP17mean);
        //print(qP17nPixels, ",", qP17mean);

//point 18
makePoint(xC[qq], yC[qq]+hC[qq]/2-thicknessin);
getRawStatistics(qP18nPixels, qP18mean);
        //print(qP18nPixels, ",", qP18mean);

//point 19
makePoint(xC[qq]+0.7*0.7*wC[qq]/2, yC[qq]+hC[qq]/2-1);
getRawStatistics(qP19nPixels, qP19mean);
        //print(qP19nPixels, ",", qP19mean);

//point 20
makePoint(xC[qq]+0.7*0.7*(wC[qq]/2-thicknessin),
yC[qq]+hC[qq]/2-thicknessin-1);
getRawStatistics(qP20nPixels, qP20mean);
        //print(qP20nPixels, ",", qP20mean);

//point 21
makePoint(xC[qq]+0.35*wC[qq]+1, yC[qq]+0.35*hC[qq]+1);
getRawStatistics(qP21nPixels, qP21mean);
        //print(qP21nPixels, ",", qP21mean);
```

```
//point 22

makePoint(xC[qq]+0.70*(wC[qq]/2-thicknessin),
yC[qq]+0.70*(hC[qq]/2-thicknessin));

getRawStatistics(qP22nPixels, qP22mean);

        //print(qP22nPixels, ",", qP22mean);


//point 23

makePoint(xC[qq]+wC[qq]/2-1, yC[qq]+0.7*0.7*hC[qq]/2);

getRawStatistics(qP23nPixels, qP23mean);

        //print(qP23nPixels, ",", qP23mean);


//point 24

makePoint(xC[qq]+(wC[qq]/2-thicknessin)-1,
yC[qq]+0.7*0.7*(hC[qq]/2-thicknessin));

getRawStatistics(qP24nPixels, qP24mean);

        //print(qP24nPixels, ",", qP24mean);


//point 25

makePoint(xC[qq]+0.35*wC[qq]+1, yC[qq]-0.35*hC[qq]-1);

getRawStatistics(qP25nPixels, qP25mean);

        //print(qP25nPixels, ",", qP25mean);


//point 26

makePoint(xC[qq]+0.70*(wC[qq]/2-thicknessin),yC[qq]-
0.70*(hC[qq]/2-thicknessin));
```

```
getRawStatistics(qP26nPixels, qP26mean);
        //print(qP26nPixels, ",", qP26mean);

//point 27
makePoint(xC[qq]+wC[qq]/2-1, yC[qq]-0.7*0.7*hC[qq]/2);
getRawStatistics(qP27nPixels, qP27mean);
        //print(qP27nPixels, ",", qP27mean);

//point 28
makePoint(xC[qq]+(wC[qq]/2-thicknessin)-1,                yC[qq]-
0.7*0.7*(hC[qq]/2-thicknessin));
getRawStatistics(qP28nPixels, qP28mean);
        //print(qP28nPixels, ",", qP28mean);

//point 29
makePoint(xC[qq]+0.35*wC[qq]+1, yC[qq]-0.35*hC[qq]-1);
getRawStatistics(qP29nPixels, qP29mean);
        //print(qP29nPixels, ",", qP29mean);

//point 30
makePoint(xC[qq]+0.70*(wC[qq]/2-thicknessin),             yC[qq]-
0.70*(hC[qq]/2-thicknessin));
getRawStatistics(qP30nPixels, qP30mean);
        //print(qP30nPixels, ",", qP30mean);

//point 31
```

```
makePoint(xC[qq]+0.7*0.7*wC[qq]/2, yC[qq]-hC[qq]/2+1);

getRawStatistics(qP31nPixels, qP31mean);

        //print(qP31nPixels, ",", qP31mean);


//point 32

makePoint(xC[qq]+0.7*0.7*(wC[qq]/2-thicknessin),          yC[qq]-
hC[qq]/2+thicknessin+1);

getRawStatistics(qP32nPixels, qP32mean);

        //print(qP32nPixels, ",", qP32mean);


if (wC[qq]<=hC[qq])

{

Perimeter = 2*3.141592658*(wC[qq]-4)+4*(hC[qq]-wC[qq]) ;

}


else    Perimeter =2*3.141592658*(hC[qq]-2)+4*(wC[qq]-hC[qq]) ;




intq=(q1nPixels*(q1mean-bC[qq])+q2nPixels*(q2mean-
bC[qq])+q3nPixels*(q3mean-bC[qq])+q4nPixels*(q4mean-
bC[qq])+q5nPixels*(q5mean-bC[qq])+q6nPixels*(q6mean-
bC[qq])+q7nPixels*(q7mean-bC[qq])+q8nPixels*(q8mean-
bC[qq])+q9nPixels*(q9mean-bC[qq])+q10nPixels*(q10mean-
bC[qq])+q11nPixels*(q11mean-bC[qq])+q12nPixels*(q12mean-
bC[qq])+q13nPixels*(q13mean-bC[qq])+q14nPixels*(q14mean-
bC[qq])+q15nPixels*(q15mean-bC[qq])+q16nPixels*(q16mean-
bC[qq]))-(qP32nPixels*(qP32mean-bC[qq])+qP31nPixels*(qP31mean-
bC[qq])+qP30nPixels*(qP30mean-bC[qq])+qP29nPixels*(qP29mean-
bC[qq])+qP28nPixels*(qP28mean-bC[qq])+qP27nPixels*(qP27mean-
```

```
bC[qq])+qP26nPixels*(qP26mean-bC[qq])+qP25nPixels*(qP25mean-
bC[qq])+qP24nPixels*(qP24mean-bC[qq])+qP23nPixels*(qP23mean-
bC[qq])+qP22nPixels*(qP22mean-bC[qq])+qP21nPixels*(qP21mean-
bC[qq])+qP20nPixels*(qP20mean-bC[qq])+qP19nPixels*(qP19mean-
bC[qq])+qP18nPixels*(qP18mean-bC[qq])+qP17nPixels*(qP17mean-
bC[qq])+qP16nPixels*(qP16mean-bC[qq])+qP15nPixels*(qP15mean-
bC[qq])+qP14nPixels*(qP14mean-bC[qq])+qP13nPixels*(qP13mean-
bC[qq])+qP12nPixels*(qP12mean-bC[qq])+qP11nPixels*(qP11mean-
bC[qq])+qP10nPixels*(qP10mean-bC[qq])+qP9nPixels*(qP9mean-
bC[qq])+qP8nPixels*(qP8mean-bC[qq])+qP7nPixels*(qP7mean-
bC[qq])+qP6nPixels*(qP6mean-bC[qq])+qP5nPixels*(qP5mean-
bC[qq])+qP4nPixels*(qP4mean-bC[qq])+qP3nPixels*(qP3mean-
bC[qq])+qP2nPixels*(qP2mean-bC[qq])+qP1nPixels*(qP1mean-
bC[qq]));


print("Cell #", qq+1, ":\t ", xC[qq], ", ", yC[qq], "\t",
Background, "\t", wC[qq], "\t", hC[qq], "\t", (hC[qq]+wC[qq])/2-
(xx+yy), "\t", Perimeter, "\t", pC[qq], "\t", vC[qq], "\t",
intq, "\t", q1nPixels+q2nPixels+q3nPixels+q4nPixels, "\t",
(q1nPixels*(q1mean-bC[qq] )+q2nPixels*(q2mean-bC[qq]
)+q3nPixels*(q3mean-bC[qq] )+q4nPixels*(q4mean-bC[qq] ))/intq,
"\t", q5nPixels+q6nPixels+q7nPixels+q8nPixels, "\t",
(q5nPixels*(q5mean-bC[qq] )+q6nPixels*(q6mean-bC[qq]
)+q7nPixels*(q7mean-bC[qq] )+q8nPixels*(q8mean-bC[qq] ))/intq,
"\t", q9nPixels+q10nPixels+q11nPixels+q12nPixels, "\t",
(q9nPixels*(q9mean-bC[qq] )+q10nPixels*(q10mean-bC[qq]
)+q11nPixels*(q11mean-bC[qq] )+q12nPixels*(q12mean-bC[qq]
))/intq, "\t", q13nPixels+q14nPixels+q15nPixels+q16nPixels,
"\t", (q13nPixels*(q13mean-bC[qq] )+q14nPixels*(q14mean-bC[qq]
)+q15nPixels*(q15mean-bC[qq] )+q16nPixels*(q16mean-bC[qq]
))/intq, "\t", q1nPixels+q2nPixels+q15nPixels+q16nPixels, "\t",
(q1nPixels*(q1mean-bC[qq] )+q2nPixels*(q2mean-bC[qq]
)+q16nPixels*(q16mean-bC[qq] )+q15nPixels*(q15mean-bC[qq]
))/intq, "\t", q14nPixels+q13nPixels+q12nPixels+q11nPixels,
"\t", (q14nPixels*(q14mean-bC[qq] )+q13nPixels*(q13mean-bC[qq]
)+q12nPixels*(q12mean-bC[qq] )+q11nPixels*(q11mean-bC[qq]
))/intq, "\t", q10nPixels+q9nPixels+q8nPixels+q7nPixels, "\t",
(q10nPixels*(q10mean-bC[qq] )+q9nPixels*(q9mean-bC[qq]
)+q8nPixels*(q8mean-bC[qq] )+q7nPixels*(q7mean-bC[qq] ))/intq,
"\t", q6nPixels+q5nPixels+q3nPixels+q4nPixels, "\t",
```

```
(q6nPixels*(q6mean-bC[qq]              )+q5nPixels*(q5mean-bC[qq]
)+q4nPixels*(q4mean-bC[qq] )+q3nPixels*(q3mean-bC[qq] ))/intq);

//print(vC[qq],     (q1nPixels*(q1mean-bC[qq])+q2nPixels*(q2mean-
bC[qq])+q3nPixels*(q3mean-bC[qq])+q4nPixels*(q4mean-
bC[qq])+q5nPixels*(q5mean-bC[qq])+q6nPixels*(q6mean-
bC[qq])+q7nPixels*(q7mean-bC[qq])+q8nPixels*(q8mean-
bC[qq])+q9nPixels*(q9mean-bC[qq])+q10nPixels*(q10mean-
bC[qq])+q11nPixels*(q11mean-bC[qq])+q12nPixels*(q12mean-
bC[qq])+q13nPixels*(q13mean-bC[qq])+q14nPixels*(q14mean-
bC[qq])+q15nPixels*(q15mean-bC[qq])+q16nPixels*(q16mean-
bC[qq]))-(qP32nPixels*(qP32mean-bC[qq])+qP31nPixels*(qP31mean-
bC[qq])+qP30nPixels*(qP30mean-bC[qq])+qP29nPixels*(qP29mean-
bC[qq])+qP28nPixels*(qP28mean-bC[qq])+qP27nPixels*(qP27mean-
bC[qq])+qP26nPixels*(qP26mean-bC[qq])+qP25nPixels*(qP25mean-
bC[qq])+qP24nPixels*(qP24mean-bC[qq])+qP23nPixels*(qP23mean-
bC[qq])+qP22nPixels*(qP22mean-bC[qq])+qP21nPixels*(qP21mean-
bC[qq])+qP20nPixels*(qP20mean-bC[qq])+qP19nPixels*(qP19mean-
bC[qq])+qP18nPixels*(qP18mean-bC[qq])+qP17nPixels*(qP17mean-
bC[qq])+qP16nPixels*(qP16mean-bC[qq])+qP15nPixels*(qP15mean-
bC[qq])+qP14nPixels*(qP14mean-bC[qq])+qP13nPixels*(qP13mean-
bC[qq])+qP12nPixels*(qP12mean-bC[qq])+qP11nPixels*(qP11mean-
bC[qq])+qP10nPixels*(qP10mean-bC[qq])+qP9nPixels*(qP9mean-
bC[qq])+qP8nPixels*(qP8mean-bC[qq])+qP7nPixels*(qP7mean-
bC[qq])+qP6nPixels*(qP6mean-bC[qq])+qP5nPixels*(qP5mean-
bC[qq])+qP4nPixels*(qP4mean-bC[qq])+qP3nPixels*(qP3mean-
bC[qq])+qP2nPixels*(qP2mean-bC[qq])+qP1nPixels*(qP1mean-
bC[qq])));

//print(vC[qq]/((q1nPixels*(q1mean-bC[qq])+q2nPixels*(q2mean-
bC[qq])+q3nPixels*(q3mean-bC[qq])+q4nPixels*(q4mean-
bC[qq])+q5nPixels*(q5mean-bC[qq])+q6nPixels*(q6mean-
bC[qq])+q7nPixels*(q7mean-bC[qq])+q8nPixels*(q8mean-
bC[qq])+q9nPixels*(q9mean-bC[qq])+q10nPixels*(q10mean-
bC[qq])+q11nPixels*(q11mean-bC[qq])+q12nPixels*(q12mean-
bC[qq])+q13nPixels*(q13mean-bC[qq])+q14nPixels*(q14mean-
bC[qq])+q15nPixels*(q15mean-bC[qq])+q16nPixels*(q16mean-
bC[qq]))-(qP32nPixels*(qP32mean-bC[qq])+qP31nPixels*(qP31mean-
bC[qq])+qP30nPixels*(qP30mean-bC[qq])+qP29nPixels*(qP29mean-
bC[qq])+qP28nPixels*(qP28mean-bC[qq])+qP27nPixels*(qP27mean-
bC[qq])+qP26nPixels*(qP26mean-bC[qq])+qP25nPixels*(qP25mean-
bC[qq])+qP24nPixels*(qP24mean-bC[qq])+qP23nPixels*(qP23mean-
```

```
bC[qq])+qP22nPixels*(qP22mean-bC[qq])+qP21nPixels*(qP21mean-
bC[qq])+qP20nPixels*(qP20mean-bC[qq])+qP19nPixels*(qP19mean-
bC[qq])+qP18nPixels*(qP18mean-bC[qq])+qP17nPixels*(qP17mean-
bC[qq])+qP16nPixels*(qP16mean-bC[qq])+qP15nPixels*(qP15mean-
bC[qq])+qP14nPixels*(qP14mean-bC[qq])+qP13nPixels*(qP13mean-
bC[qq])+qP12nPixels*(qP12mean-bC[qq])+qP11nPixels*(qP11mean-
bC[qq])+qP10nPixels*(qP10mean-bC[qq])+qP9nPixels*(qP9mean-
bC[qq])+qP8nPixels*(qP8mean-bC[qq])+qP7nPixels*(qP7mean-
bC[qq])+qP6nPixels*(qP6mean-bC[qq])+qP5nPixels*(qP5mean-
bC[qq])+qP4nPixels*(qP4mean-bC[qq])+qP3nPixels*(qP3mean-
bC[qq])+qP2nPixels*(qP2mean-bC[qq])+qP1nPixels*(qP1mean-
bC[qq])))));

//print( q1nPixels+ q2nPixels+ q3nPixels+ q4nPixels,  q5nPixels+
q6nPixels+   q7nPixels+   q8nPixels,     q9nPixels+   q10nPixels+
q11nPixels+  q12nPixels,    q13nPixels+  q14nPixels+  q15nPixels+
q16nPixels);

//print(    q1nPixels+    q2nPixels+    q15nPixels+    q16nPixels,
q3nPixels+   q4nPixels+   q5nPixels+   q6nPixels,      q7nPixels+
q8nPixels+   q9nPixels+   q10nPixels,     q13nPixels+   q14nPixels+
q11nPixels+ q12nPixels);

//print( "Cell  #", qq+1, ":\t  ", xC[qq], ", ", yC[qq], "\t",
vC[qq],   "\t",   tC[qq],   "\t",   wC[qq],   "\t",   hC[qq],   "\t",
(hC[qq]+wC[qq])/2-(xx+yy));

//print( "Cell  #", qq+1, ":\t  ", xC[qq], ", ", yC[qq], "\t",
vC[qq],   "\t",   tC[qq],   "\t",   wC[qq],   "\t",   hC[qq],   "\t",
(hC[qq]+wC[qq])/2-(xx+yy),       "\t",       q1nPixels,       "\t",
q1nPixels*(q1mean-bC[qq]     ),     "\t",     q2nPixels,     "\t",
q2nPixels*(q2mean-bC[qq]       ),       "\t",q3nPixels,       "\t",
q3nPixels*(q3mean-bC[qq]       ),"\t",       q4nPixels,       "\t",
q4nPixels*(q4mean-bC[qq]    ),    "\t",    q5nPixels,        "\t",
q5nPixels*(q5mean-bC[qq]         ),         "\t",         q6nPixels,
"\t",q6nPixels*(q6mean-bC[qq]           ),"\t",          q7nPixels,
"\t",q7nPixels*(q7mean-bC[qq]       ),       "\t",       q8nPixels,
"\t",q8nPixels*(q8mean-bC[qq]          ),"\t",          q9nPixels,
"\t",q9nPixels*(q9mean-bC[qq]       ),       "\t",       q10nPixels,
"\t",q10nPixels*(q10mean-bC[qq]     ),     "\t",     q11nPixels,
"\t",q11nPixels*(q11mean-bC[qq]     ),     "\t",     q12nPixels,
"\t",q12nPixels*(q12mean-bC[qq]  ));/print(  "Q1+Q2+Q3:  ",  "\t",
q1nPixels*(q1mean-bC[qq]               )+q2nPixels*(q2mean-bC[qq]
```

```
)+q3nPixels*(q3mean-bC[qq]     ),     "\tQ4+Q5+Q6:     ",     "\t",
q4nPixels*(q4mean-bC[qq]                )+q5nPixels*(q5mean-bC[qq]
)+q6nPixels*(q6mean-bC[qq]     ),     "\tQ7+Q8+Q9:     ",     "\t",
q7nPixels*(q7mean-bC[qq]                )+q8nPixels*(q8mean-bC[qq]
)+q9nPixels*(q9mean-bC[qq]    ),    "\tQ10+Q11+Q12:    ",    "\t",
q10nPixels*(q10mean-bC[qq]           )+q11nPixels*(q11mean-bC[qq]
)+q12nPixels*(q12mean-bC[qq] ));

//print(    "Q2+Q3+Q4:    ",    "\t",    q2nPixels*(q2mean-bC[qq]
)+q3nPixels*(q3mean-bC[qq]      )+q4nPixels*(q4mean-bC[qq]      ),
"\tQ5+Q6+Q7:       ",       "\t",       q5nPixels*(q5mean-bC[qq]
)+q6nPixels*(q6mean-bC[qq]      )+q7nPixels*(q7mean-bC[qq]      ),
"\tQ8+Q9+Q10:     ",     "\t",          q8nPixels*(q8mean-bC[qq]
)+q9nPixels*(q9mean-bC[qq]     )+q10nPixels*(q10mean-bC[qq]     ),
"\tQ11+Q12+Q1:     ",     "\t",         q11nPixels*(q11mean-bC[qq]
)+q12nPixels*(q12mean-bC[qq] )+q1nPixels*(q1mean-bC[qq] ));

//print(    "Q3+Q4+Q5:    ",    "\t",    q3nPixels*(q3mean-bC[qq]
)+q4nPixels*(q4mean-bC[qq]      )+q5nPixels*(q5mean-bC[qq]      ),
"\tQ6+Q7+Q8:       ",       "\t",       q6nPixels*(q6mean-bC[qq]
)+q7nPixels*(q7mean-bC[qq]      )+q8nPixels*(q8mean-bC[qq]      ),
"\tQ9+Q10+Q11:     ",     "\t",          q9nPixels*(q9mean-bC[qq]
)+q10nPixels*(q10mean-bC[qq]    )+q11nPixels*(q11mean-bC[qq]    ),
"\tQ12+Q1+Q2:     ",     "\t",          q12nPixels*(q12mean-bC[qq]
)+q1nPixels*(q1mean-bC[qq] )+q2nPixels*(q2mean-bC[qq] ));

//print(vC[qq],         "\t",                  q1nPixels*(q1mean-
bC[qq])+q2nPixels*(q2mean-bC[qq])+q3nPixels*(q3mean-
bC[qq])+q4nPixels*(q4mean-bC[qq])+q5nPixels*(q5mean-
bC[qq])+q6nPixels*(q6mean-bC[qq])+q7nPixels*(q7mean-
bC[qq])+q8nPixels*(q8mean-bC[qq])+q9nPixels*(q9mean-
bC[qq])+q10nPixels*(q10mean-bC[qq])+q11nPixels*(q11mean-
bC[qq])+q12nPixels*(q12mean-bC[qq])+q13nPixels*(q13mean-
bC[qq])+q14nPixels*(q14mean-bC[qq])+q15nPixels*(q15mean-
bC[qq])+q16nPixels*(q16mean-bC[qq]));

//print(vC[qq]/(q1nPixels*(q1mean-bC[qq])+q2nPixels*(q2mean-
bC[qq])+q3nPixels*(q3mean-bC[qq])+q4nPixels*(q4mean-
bC[qq])+q5nPixels*(q5mean-bC[qq])+q6nPixels*(q6mean-
bC[qq])+q7nPixels*(q7mean-bC[qq])+q8nPixels*(q8mean-
bC[qq])+q9nPixels*(q9mean-bC[qq])+q10nPixels*(q10mean-
bC[qq])+q11nPixels*(q11mean-bC[qq])+q12nPixels*(q12mean-
bC[qq])+q13nPixels*(q13mean-bC[qq])+q14nPixels*(q14mean-
```

```
bC[qq])+q15nPixels*(q15mean-bC[qq])+q16nPixels*(q16mean-
bC[qq])));

//print(q1nPixels+q2nPixels+q3nPixels+q4nPixels+q5nPixels+q6nPix
els+q7nPixels+q8nPixels+q9nPixels+q10nPixels+q11nPixels+q12nPixe
ls+q13nPixels+q14nPixels+q15nPixels+q16nPixels, ",", q1nPixels,
q2nPixels, q3nPixels, q4nPixels, q5nPixels, q6nPixels,
q7nPixels, q8nPixels, q9nPixels, q10nPixels, q11nPixels,
q12nPixels, q13nPixels, q14nPixels, q15nPixels, q16nPixels);

}


setKeyDown("shift");

          for( r=0; r<celltotal; r++ )

               makePoint(xC[r], yC[r]);

          setKeyDown( "none" );


          //print( "Cells Found in ", paths[q], ": ",
celltotal);

          print( "" );

          selectWindow("Results");

          run("Close");

          if( ci == "After Each Image is Scanned" )

          {

               selectWindow( File.getName(paths[q]) );

               run("Close");

          }

     }

     if( ci == "After all Images are Scanned" ){
```

```
          waitForUser( "Hit OK to close all images and return to
Menu" );
          for( q=0; q<i; q++ )
          {
               selectWindow( File.getName(paths[q]) );
               run("Close");
          }
     }
}
```

// For each image, the background was first chosen by default method in Image J program. The user was free to choose the proper background method based on research requirements. First of all, a circle of similar size of leukemia cell was initiated, it moved along the image by certain path and paused if it detected a bright point. Set up this bright point as a point in an axis system, another 32 points were measured. Once there were over 60% of those points passing the threshold, two polygons (circles) were draw by connecting them together. Those two polygons enclosed the bright area of the cell where fluorophore-labelled antibodies binding to the target surface markers. By analyze the intensities of the cell rings, user can estimate the surface marker amount on the cells. Also, the diameter of the polygon (circle) gave the measurements of the cells.

```
function Preferences()
{
     print( "Preferences/Options in Operation" );

     Dialog.create( "Shan - Preferences/Options" );
     Dialog.addNumber( "Minimum Cell Length: ", length );
     Dialog.addNumber( "Maximum Cell Length: ", maxlength );
```

```
     Dialog.addNumber( "Cell Thickness IN: ", thicknessin );
     Dialog.addNumber( "Cell Thickness OUT: ", thicknessout );
     Dialog.addCheckbox(       "Show       all       thresholds",
showallthresholds);
     Dialog.addCheckbox( "Show detailed log", logdet );
     Dialog.addChoice( "Close Images: ", closeimage, ci);



     for( mm=0; mm<thresholdmethods.length; mm++)
          Dialog.addCheckbox(               thresholdmethods[mm],
usethresholdmethod[mm] );


     Dialog.show();


     length = Dialog.getNumber();
     maxlength = Dialog.getNumber();
     thicknessin = Dialog.getNumber();
     thicknessout = Dialog.getNumber();
     showallthresholds = Dialog.getCheckbox();
     logdet = Dialog.getCheckbox();
     ci = Dialog.getChoice();


     for( mm=0; mm<thresholdmethods.length; mm++)
          usethresholdmethod[mm] = Dialog.getCheckbox();


     print( "Changes Saved" );
```

```
     print( "" );
}

function AOW()
{
     waitForUser( "Access Other Windows", "Select OK to return
to Menu" );
}

////////

////////

function FindBackground()
{

     setAutoThreshold(backgroundthresholdmethod);
     run("Analyze    Particles...",    "size=0-Infinity    pixel
circularity=0.00-1.00 show=Nothing display clear");

     high=0;
     highelement=0;

     for (r=0; r<nResults; r++) {
          if( high < getResult( "Area", r )){
```

```
                high =  getResult( "Area", r );
                highelement = r;
            }
        }

    return  getResult(  "Mean",  highelement  )+  2*getResult(
"StdDev", highelement );
}
```

APPENDIX C: Copyright Compliance

JOHN WILEY AND SONS LICENSE
TERMS AND CONDITIONS

Apr 22, 2014

This is a License Agreement between Suli Niu ("You") and John Wiley and Sons ("John Wiley and Sons") provided by Copyright Clearance Center ("CCC"). The license consists of your order details, the terms and conditions provided by John Wiley and Sons, and the payment terms and conditions.

All payments must be made in full to CCC. For payment instructions, please see information listed at the bottom of this form.

License Number

3374420657939

License date

Apr 22, 2014

Licensed content publisher

John Wiley and Sons

Licensed content publication

Microscopy Research and Technique

Licensed content title

Morphology and expression status investigations of specific surface markers on B-cell chronic lymphocytic leukemia cells

Licensed copyright line

Licensed content author

Suli Niu,Ryan Chan,Pierre Berini,Chen Wang,Shan Zou

Licensed content date

Aug 20, 2013

Start page

1147

End page

1153

Type of use

Dissertation/Thesis

Requestor type

Author of this Wiley article

Format

Electronic

Portion

Full article

Will you be translating?

No

Title of your thesis / dissertation

Morphology and expression status investigations of specific surface markers on B-cell chronic lymphocytic leukemia cells

Expected completion date

Apr 2014

Expected size (number of pages)

7

Total

0.00 USD